Jadeitite in the Syum-Keu ultramafic complex from Polar Urals, Russia: insights into fluid activity in subduction zones

Fancong Meng[1],*, Huai-Jen Yang[2], Alexander B. Makeyev[3], Yufeng Ren[1], Ksenia V. Kulikova[4]
and Natasha. I. Bryanchaninova[5]

[1]Institute of Geology, Chinese Academy of Geological Sciences (CAGS), Beijing 100037, China
*Corresponding author, e-mail: mengfancong@yeah.net
[2]Department of Earth Sciences, National Cheng-Kung University, Tainan 70101, Taiwan
[3]Institute of Geology of Ore Deposits, Petrography, Mineralogy, and Geochemistry, Russian Academy of Sciences
(IGEM RAS), Moscow 119017, Russia
[4]Institute of Geology, Komi Science Center of Uralian Division, RAS, Syktyvkar 167982, Russia
[5]State Geological Museum (SGM RAS), Moscow 119005, Russia

Abstract: New major, trace and rare earth element (REE) data, and Sr-Nd isotopic compositions of jadeitite and REE-Hf-O isotopic compositions of zircon in jadeitite of the Syum-Keu ultramafic complex of the Polar Urals are used to constrain its origin and source.

The jadeitites have high contents of Na_2O (12.80–14.56 wt%), Al_2O_3 (20.30–23.81 wt%), SiO_2 (58.47–59.50 wt%), and are enriched in Sr, Ba, Zr, Hf and depleted in Nb relative to primitive mantle values. Chondrite-normalized REE patterns of the jadeitite display weakly U-shaped distribution patterns, with La_N/Yb_N ratios of 0.82–2.42, and very weak positive Eu anomalies ($\delta Eu = 1.2$–1.6). The initial Sr isotopic compositions of the jadeitite range from 0.704000 to 0.703519 ($t = 368$ Ma), and the initial Nd-isotope ratios ($\varepsilon_{Nd} = +0.77$ to +5.61) differ from those of ancient ocean water, oceanic sediments and eclogite, metagranite, and metasediments in the nearby Marun-Keu complex.

Zircons from the jadeitite have variable REE contents (37–587 ppm) and are enriched in HREE, with La_{CN}/Yb_{CN} ratios ranging from 0.001 to 0.01, and Lu_{CN}/Gd_{CN} ratios ranging from 10 to 83. Cerium shows positive anomalies with Ce/Ce* values ranging from 2.8 to 72, and δEu from 0.53 to 1.02. The $^{176}Hf/^{177}Hf$ ratios of the zircons range from 0.282708 to 0.283017, with initial Hf isotope compositions ranging from 6.5 to 17.4. These characteristics resemble those of zircons from depleted mantle-derived magmas. The $\delta^{18}O$ isotope compositions of the zircons range from 5.03‰ to 6.04‰, with an averaged value of 5.45 ± 0.11‰, similar to those of mantle rocks, suggesting that the zircons were acquired from precursor igneous rocks, and then transported and reworked by fluids from the subducting slab. Our new results show that the jadeitite was precipitated from material mainly produced by fluid interaction with mafic-ultramafic rocks in a subduction zone environment.

Key-words: jadeitite, geochemistry, zircon, Hf-O isotope, fluids in subduction zone, Polar Urals, Russia.

1. Introduction

The global distribution of jadeitites indicates a genetic association with subduction/collision processes (Harlow & Sorensen, 2005). They commonly occur as enclaves or veins within serpentinized peridotite associated with ophiolites. Recent studies suggest that jadeitites may be divided into R-type (replacement) and P-type (precipitation) varieties (Tsujimori & Harlow, 2012; Flores *et al.*, 2013). Most researchers considered that the R-type jadeitites formed by recrystallization of subducted oceanic crust, as indicated by remnants of pyroxene and zircon (*e.g.*, Dobretsov & Ponomareva, 1965; Shi *et al.*, 2003; Harlow & Sorensen, 2005; Shi *et al.*, 2005; Shigeno *et al.*, 2005; Fu *et al.*, 2010; Compagnoni *et al.*, 2012; Tsujimori & Harlow, 2012), or by interaction between

fluids and the protolith minerals (Shigeno *et al.*, 2005). In contrast, jadeitites characterized by oscillatory mineral zoning, fluid inclusions, and a lack of relic minerals, have been attributed to precipitation from Na-Al-Si rich fluids (the P-type variety) (Sorensen *et al.*, 2006; Meng *et al.*, 2007; Morishita *et al.*, 2007; Garcia-Casco *et al.*, 2009; Yui *et al.*, 2010). However, the source of P-type jadeitites is not well constrained. For instance, seawater and fluids released by dehydration of subducting oceanic crust are potential sources of Na-Al-Si fluids produced by dehydration of sediments in subduction zones (Harlow & Sorensen, 2005), and these can interact with felsic or mafic tectonic blocks associated with ultramafic rocks (Yui *et al.*, 2010). Discoveries of Ba-rich feldspar and spherules of pure iron in some jadeitites, as well as their Li-isotopic compositions, suggest that they were derived

from subducting sediments (Morishita, 2005; Shi *et al.*, 2010, 2011; Simons *et al.*, 2010). Although zircons are common in jadeitites, it has been difficult to define their origin (Shi *et al.*, 2008; Qiu *et al.*, 2009; Fu *et al.*, 2010; Yui *et al.*, 2010, 2012, 2013; Flores *et al.*, 2013).

This paper reports new geochemical data and Sr-Nd isotopic compositions of jadeitite samples from the Syum-Keu complex, Polar Urals, Russia, as well as REE and Hf-O isotope data of the associated zircons to constrain the source of the jadeitite.

2. Geological background

The Polar Urals are located in the northernmost part of the Urals orogenic belt (Fig. 1a), where remnants of both the East European plate and West Siberian plate are preserved (Savelieva & Nesbitt, 1996; Puchkov, 2009). The study area lies in the northern end of the Polar Urals (Fig. 1b), a region of arc–continent collision (Puchkov, 2009). The western portion belongs to the East European continental margin, consisting of Paleozoic sedimentary rocks (P_Z), greenschist-facies metasedimentary rocks (Niaroveyskaya Suite) and

high-pressure gneiss (Marun-Keu complex [MK]) with eclogites and blueschists (*e.g.*, Udovkina, 1985; Dobretsov, 1991; Molina *et al.*, 2002, 2004; Glodny *et al.*, 2003, 2004). The eastern part of the orogen is a relic of oceanic lithosphere, which was obducted westward onto the Niaroveyskaya Suite. This region is characterized by the occurrence of ultramafic rocks (Syum-Keu complex [SK]), composed of a complicated association of dunite-wehrlite-clinopyroxenite, gabbro and metagabbro (Malyko), minor Paleozoic granodiorites and granites, and Mesozoic sedimentary cover (Mz), all thought to represent an ophiolite assemblage (*e.g.*, Moldavantsev & Kazak, 1977; Makeyev *et al.*, 1985; Shmelev, 1991; Kulikova, 2005; Savelieva & Suslov, 2014).

2.1. The Marun-Keu (MK) complex

The MK complex is hosted in the greenschist-facies metasedimentary rocks (Niaroveyskaya Suite) (Fig. 1b). It is a high-pressure suite consisting of blueschists, felsic gneisses, garnet amphibolites and eclogites (Udovkina, 1985; Dobretsov, 1991; Molina *et al.*, 2002, 2004; Glodny *et al.*, 2003, 2004). The peak metamorphic temperatures and pressures
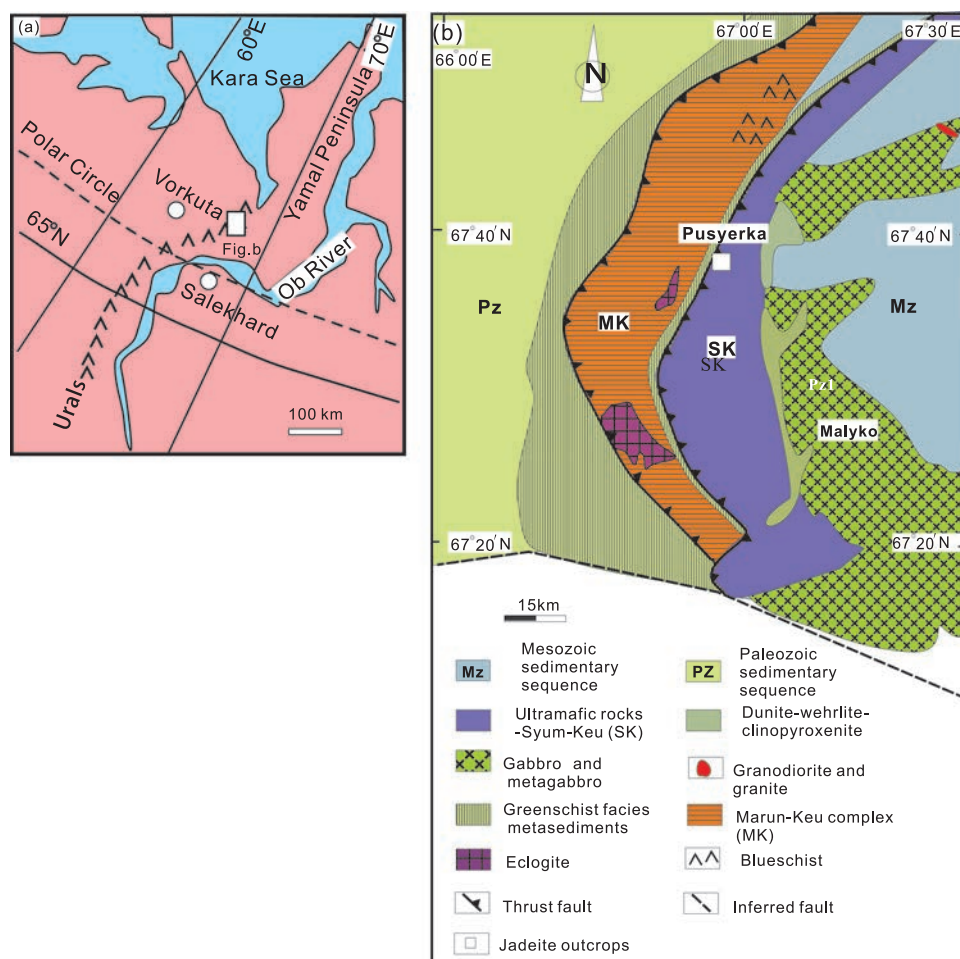

Fig. 1. Simplified geological map of the Marun-Keu complex (MK) and Syum-Keu complex (SK) in the Polar Urals (modified after Makeyev *et al.*, 1985; Udovkina, 1985; Shmelev, 1991; Kulikova, 2005). (online version in colour)

of the blueschists in the northern segment were 500 ºC and 10–11 kbar (Dobretsov & Sobolev, 1984), whereas the eclogites in the central and southern segments experienced somewhat higher temperatures (600–650 ºC) and pressures (14–17 kbar) (Udovkina, 1985; Molina *et al.*, 2002). The metamorphic ages of the eclogites are 360–355 Ma (Shatsky *et al.*, 2000; Glodny *et al.*, 2003, 2004). The MK complex has been considered as either part of the subducted East European continental margin (Glodny *et al.*, 2003, 2004), or the product of collision between the passive East European plate and the subducted Paleo-Urals oceanic lithosphere (Dobretsov, 1991).

2.2. The Syum-Keu (SK) complex

The SK complex occurs as a NE-trending block about 60 km long and 12–15 km wide, that crops out over an area of ~ 600 km^2. Based on its occurrence and geophysical data, the thickness of the complex is estimated to vary from 1 km on the west side to 3 km on the east (Fig. 1b). It is composed mainly of lherzolite, dunite and harzburgite, with lherzolite–harzburgite occurring predominantly in the west and dunite–harzburgite in the east (Moldavantsev & Kazak, 1977; Makeyev *et al.*, 1985; Shmelev, 1991, 2011; Gurskaya & Smelova, 2003; Savelieva & Suslov, 2014). These rocks contain a few conformable veins of websterite, and both ortho- and clinopyroxenite, which underwent intense ductile deformation during emplacement (Shmelev, 1991; Savelieva & Suslov, 2014). The entire complex is variably serpentinized (45–65 vol%) (Makeyev, 1992). A Sm–Nd mineral isochron age of 523 ± 10 Ma has been obtained from the harzburgite (Andreichev, 2004). On the basis of its geological, mineralogical and geochemical character, the SK complex is considered to be part of a Suprasubduction zone-type ophiolite (Shmelev, 2011), specifically a mantle section of the ophiolite allochthon (Savelieva & Suslov, 2014).

The crustal section on the eastern side is composed of layered dunite, wehrlite, clinopyroxenite, Malyko gabbro, and metagabbro with a few plagiogranites. The gabbros were formed in a back-arc basin or an island arc environment (Kulikova, 2005). Zircons from lenses of plagiogranite in the metagabbro yielded a U–Pb age of 451 ± 14Ma (Andreichev, 2004), which was interpreted as the age of the oceanic crust. The crust and mantle sections are not genetically linked by a simple melt–residue relationship, and the contact between the SK complex and cumulate mafic-ultramafic rocks is unclear. Some workers believe that the ophiolite sequence was inverted and thrust eastward to form the garnet-bearing amphibolite (metagabbro) below the SK complex (Kulikova, 2005). Others have proposed that it represents the crust–mantle transition zone with the gabbro overlying the mantle peridotite (Savelieva & Suslov, 2014).

2.3. Occurrences of jadeitite

The Pusyerka jadeitites occur as veins or lenses in the base of the peridotite on the west side of the SK complex, where they were first mined in 1980 (Fig. 1b). Jadeite

mineralization took place in the serpentinized dunite-harzburgite wall rock (Fig. 2a, b) and is in fault contact with dunite-harzburgite, dipping 50–70° SE (Fishman, 2006; Meng *et al.*, 2011). In the strongly serpentinized segment, there are numerous jadeitite veins, striking N30°E (Fig. 2a). The abundance of jadeitite veins increases from NE to SW. The veins are 20–100 m thick and extend along strike for up to about 10 km. More than 70 jadeitite bodies have been identified. They are mainly brecciated blocks of eluvial or slope deposits. Primary veins are exposed locally (Fishman, 2006), and are hosted directly in dark serpentinite composed mainly of antigorite, brucite, and magnetite, with minor anthophyllite and phlogopite (Makeyev, 1992). These characteristics of the Pusyerka jadeitite bodies resemble those of the Levoketchpel deposits at Voykar-Synisky in the Polar Urals (*e.g.*, Dobretsov & Ponomareva, 1965; Harlow & Sorensen, 2005). The jadeitite consists mainly of jadeite (Jd$_{85-88}$), with minor omphacite (Jd$_{54-74}$) and zircon (Fig. 2c). Oscillatory zoning (Fig. 2d) and fluid inclusions are well developed in the jadeite (Meng *et al.*, 2007, 2011). Zircon SHRIMP dating yielded a weighted mean ^{206}Pb/^{238}U age of 404 ±7 Ma for the jadeitite, with the youngest age being 368 ± 11 Ma (Meng *et al.*, 2011).

3. Analytical methods

All jadeitite samples were collected from loose blocks of the same vein (Fig. 2a), and the zircons were separated from jadeitite sample Y5-100 (Meng *et al.*, 2011). Abundances of whole-rock major elements were determined by XRF (using 3080E) and ICP-MS (Excell) at the National Research Center for Geoanalysis (NRCG), Chinese Academy of Geological Sciences (CAGS) in Beijing, with a precision better than 2 % for all oxides. Trace element abundances of whole-rock samples were measured by ICP-MS (Excell) with a precision of 5–8 %. Strontium and Nd isotopic compositions were determined by thermal ionization spectrometry (MAT262) at the Department of Earth Sciences, National Cheng-Kung University, Taiwan, following the procedures of Tseng *et al.* (2009).

Zircon and jadeite were analyzed for trace element abundances using LA-ICP-MS (Thermo Element II + New Wave UP213) at the NRCG, CAGS, in Beijing. The spot size is about 40 μm in diameter, and the detailed analytical procedures are described by Hu *et al.* (2008). The Lu-Hf isotopic compositions of zircon were measured *in situ* with a Geolas-193 laser ablation microprobe, which is attached to a Neptune multi-collector ICP-MS at the Institute of Mineral Resources (IMR), CAGS. The analytical procedures are described by Hou *et al.* (2007). Calculation of Hf-model ages (T$_{DM}$) is based on a depleted-mantle source with a present-day ^{176}Hf/^{177}Hf = 0.28325, using a ^{176}Lu decay constant of 1.865×10^{-11} year^{-1} (Scherer *et al.*, 2001). The εHf(t) values were calculated from zircon U-Pb ages and the chondritic ^{176}Hf/^{177}Hf and ^{176}Lu/^{177}Hf values of 0.282772 and 0.0332, respectively (Blichert-Toft & Albarède, 1997). Oxygen isotopic compositions of
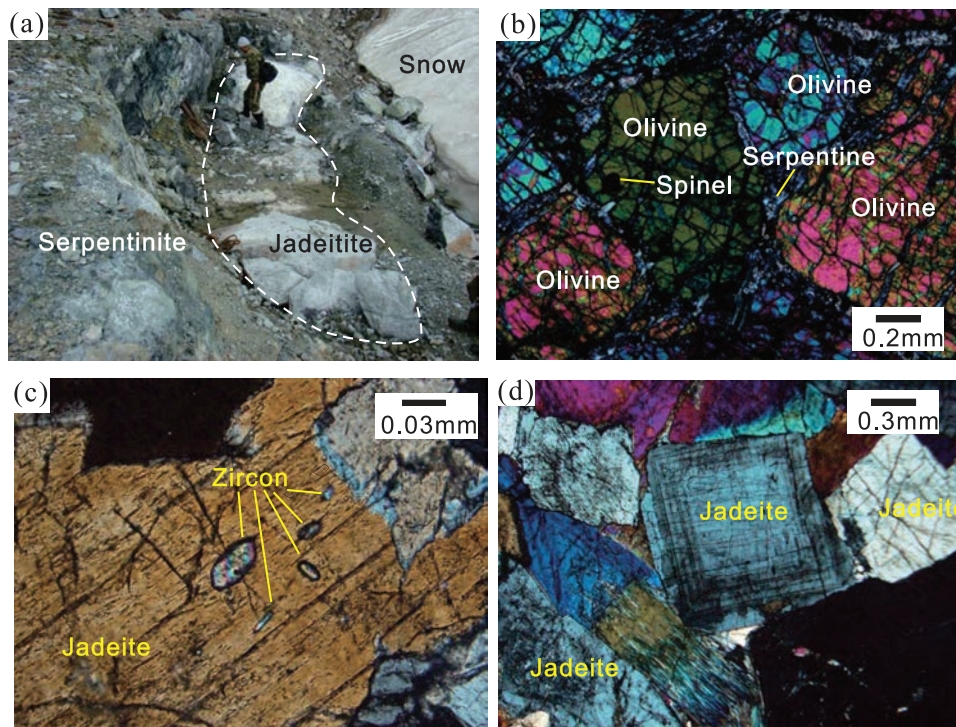
Fig. 2. Occurrence and photomicrographs of Pusyerka jadeitite from the Polar Urals (a) Jadeitite veins in serpentinite; size of vein is 10 × 2 m; (b) Dunite composed of olivine + spinel, as wall-rock of the jadeitite; (c) Zircons in jadeite; (d) Jadeitite with coarse-grained texture; some jadeite with concentric and oscillatory zoning. (online version in colour)

zircon were measured *in situ* at the Institute of Geology and Geophysics (IGG), Chinese Academy of Sciences (CAS), using a CAMECA IMS 1280 with a ~2 nA primary Cs^+ ion beam accelerated to 10 kV. The analytical procedures were the same as those described by Li *et al.* (2010a). The spot size is about 20 μm in diameter, including 10 μm beam diameter and 10 μm raster. Negative secondary $^{18}O^-$ and $^{16}O^-$ ions were extracted at 10 kV and measured in multicollector mode using two off-axis Faraday cups with an intensity of ^{16}O typically at 1×10^9 cps. Each analysis was run in the sequence of pre-sputtering for 2 min, automatic beam centering for 1 min, and 80 s (20 cycles) of data collection. Oxygen isotope ratios are expressed as $\delta^{18}O$, representing deviation of measured $^{18}O/^{16}O$ values from the Vienna standard mean ocean water (VSMOW) in per mil. All data were then corrected based on the Temora 2 value of 8.20 ‰ (Black *et al.*, 2004). Uncertainties on individual analyses are usually better than 0.2 ‰ − 0.3 ‰ (1σ). The same spots were targeted for U–Pb age determination wherever possible.

4. Results

4.1. Major elements

Five jadeitite samples have similar major-element compositions, with SiO_2, Al_2O_3, and Na_2O contents varying in the ranges of 58.5–59.5 %, 20.3–23.8 %, and 12.8–14.6 %,

respectively. These data are compared to those of oceanic gabbro and diabase from the Voykar ophiolite and other rocks from the Marun-Keu complex (Table 1, Fig. 3a, b). The jadeitite samples are characterized by the highest Na_2O and Al_2O_3 abundances among all the samples, with their SiO_2 contents lower than those of the metagranite and metasediment samples.

4.2. Trace elements

The jadeitite samples have very low rare earth element (REE) contents, varying from 1.13 to 5.42 ppm (Table 1, Fig. 4a), and patterns of four samples are lower than chondrite (except sample M-18). All samples show slightly concave chondrite-normalized REE patterns, with slight enrichment in both LREE and HREE and with small positive Eu anomalies (δEu = 1.12-1.60); La_{CN}/Sm_{CN} ratios vary from 0.26 to 2.06 and La_{CN}/Yb_{CN} ratios from 0.82 to 2.42. These distribution patterns are similar to those of the microgabbro and diabase from the Voykar ophiolite, with the jadeitite samples having relatively lower REE abundances (Fig. 4a).

In the primitive-mantle-normalized spidergram (Fig. 4b), the jadeitite samples are notably enriched in Ba, U, Sr, Zr and Hf, with sample M-18 showing the highest enrichment in these elements. Uranium and Zr abundances are higher than the primitive mantle values by factors of 20 and 50, respectively, displaying strong crustal signatures (Rollinson, 1993). The extents of Nb and Ta depletions in these jadeitite samples are similar to those of arc volcanic rocks (Wlison, 1989).

Table 1. Major (wt%), REE and trace element (ppm) contents of jadeitite from Syum-Keu (SK), Polar Urals, Russia.

Samples	M-18	M-18-1	M-18-2	M-18-4	Y5-100
SiO_2	58.47	59.5	59.21	58.65	58.69
TiO_2	0.07	0.04	0.05	0.05	0.05
Al_2O_3	20.3	23.81	23.03	21.22	21.7
Fe_2O_3	1.05	0.21	0.38	0.88	0.69
FeO	0.23	0.27	0.23	0.27	0.23
MnO	0.02	0.01	0.01	0.02	0.02
MgO	2.8	0.51	0.88	2.35	1.93
CaO	3.75	0.79	1.3	3.12	2.69
Na_2O	12.8	14.56	14.06	12.9	13.39
K_2O	0.03	0.02	0.02	0.02	0.02
P_2O_5	0.01	0.01	0	0.01	0.01
CO_2	0.16	0.11	0.12	0.16	0.15
H_2O^+	0.38	0.3	0.52	0.24	0.23
LOI	0.7	0.58	0.64	0.53	0.54
La	0.56	0.16	0.14	0.26	0.17
Ce	1.76	0.42	0.38	0.89	0.58
Pr	0.23	0.05	0.05	0.13	0.09
Nd	1.14	0.21	0.22	0.68	0.53
Sm	0.29	0.05	0.06	0.16	0.17
Eu	0.10	0.02	0.02	0.06	0.06
Gd	0.26	0.05	0.05	0.13	0.16
Tb	0.04	0.01	0.01	0.02	0.03
Dy	0.33	0.05	0.07	0.12	0.23
Ho	0.08	0.01	0.02	0.03	0.05
Er	0.24	0.03	0.04	0.07	0.14
Tm	0.04	0.01	0.01	0.01	0.02
Yb	0.31	0.06	0.06	0.07	0.14
Lu	0.05	0.01	0.01	0.01	0.02
$\sum REE$	5.42	1.14	1.13	2.63	2.39
La_{CN}/Sm_{CN}	1.21	2.06	1.46	1.04	0.62
La_{CN}/Yb_{CN}	1.22	1.86	1.59	2.42	0.82
δEu	1.12	1.60	1.13	1.33	1.15
Rb	0.75	0.69	0.79	0.15	0.41
Sr	229	65	91	400	137
Ba	12.37	50.65	9.90	22.75	2.70
Cs	0.07	0.02	0.02	0.00	0.02
Zr	637.0	27.0	30.3	43.6	73.2
Hf	18.03	0.74	0.91	1.16	1.82
Nb	0.12	0.19	0.17	0.05	0.05
Ta	0.01	0.02	0.04	0.01	0.01
U	0.32	0.02	0.02	0.02	0.03
Th	0.21	0.08	0.06	0.03	0.06
Pb	0.20	0.20	0.21	0.07	0.19
Sc	1.30	0.24	0.22	1.02	0.35
Ti	443	317	402	353	369
V	34.96	45.41	54.92	17.08	25.59
Cr	255	14	39	105	20
Co	4.61	2.51	2.50	3.46	3.83
Ni	71.88	6.55	14.49	46.46	52.58
Cu	4.00	6.79	6.80	4.73	6.17
Zn	5.45	6.48	5.63	5.65	6.10
Y	2.74	0.46	0.54	0.91	1.65

Note: Major element analyses performed in National Research Center of Geoanalysis (Beijing);
Trace elements analyses performed in Department of earth sciences, National Cheng-kung University, Tainan, Taiwan

4.3. Sr-Nd isotopes

The $^{87}Sr/^{86}Sr$ and $^{143}Nd/^{144}Nd$ ratios of the five jadeitite samples vary from 0.70345 to 0.70360 and from 0.51257 to 0.51293, respectively (Tables 2 and 3). Calculated to the formation age of 368 ± 11 Ma (Meng *et al.*, 2011), the initial $(^{87}Sr/^{86}Sr)_i$ and $\epsilon_{Nd}(368)$ are in the ranges of 0.70340–0.70352 and 0.77–5.61, respectively (Figs 5 and 6).

4.4. Trace elements of zircon

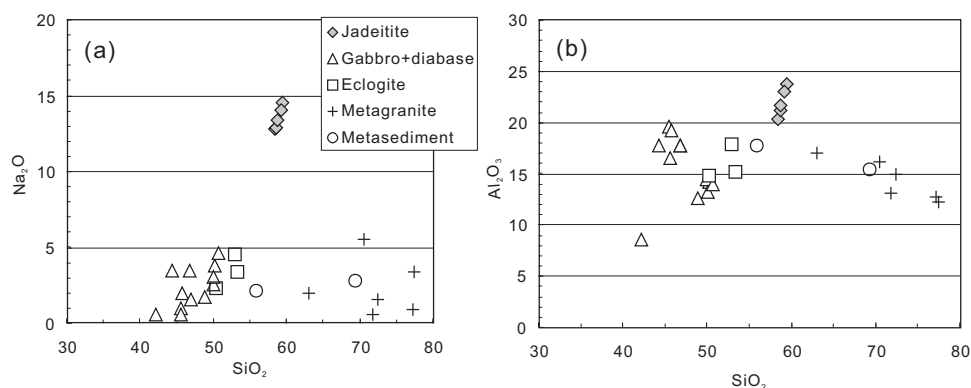Seventeen LA-ICP-MS trace-element analyses were carried out on zircon grains from sample Y5-100 (Table 4,

Fig. 3. Plots of SiO₂ *vs.*Al₂O₃ contents (a), and SiO₂ *vs.*Na₂O contents (b) in jadeitite. Also shown for comparison are compositions of the Marun-Keu complex, including eclogite, metagranite and metasediment (after Molina *et al.*, 2002; Glodny *et al.*, 2003, 2004), and gabbro + diabase from the Voykar ophiolite, which represents inferred oceanic crust of Polar Urals (Saveliev *et al.*, 1999).
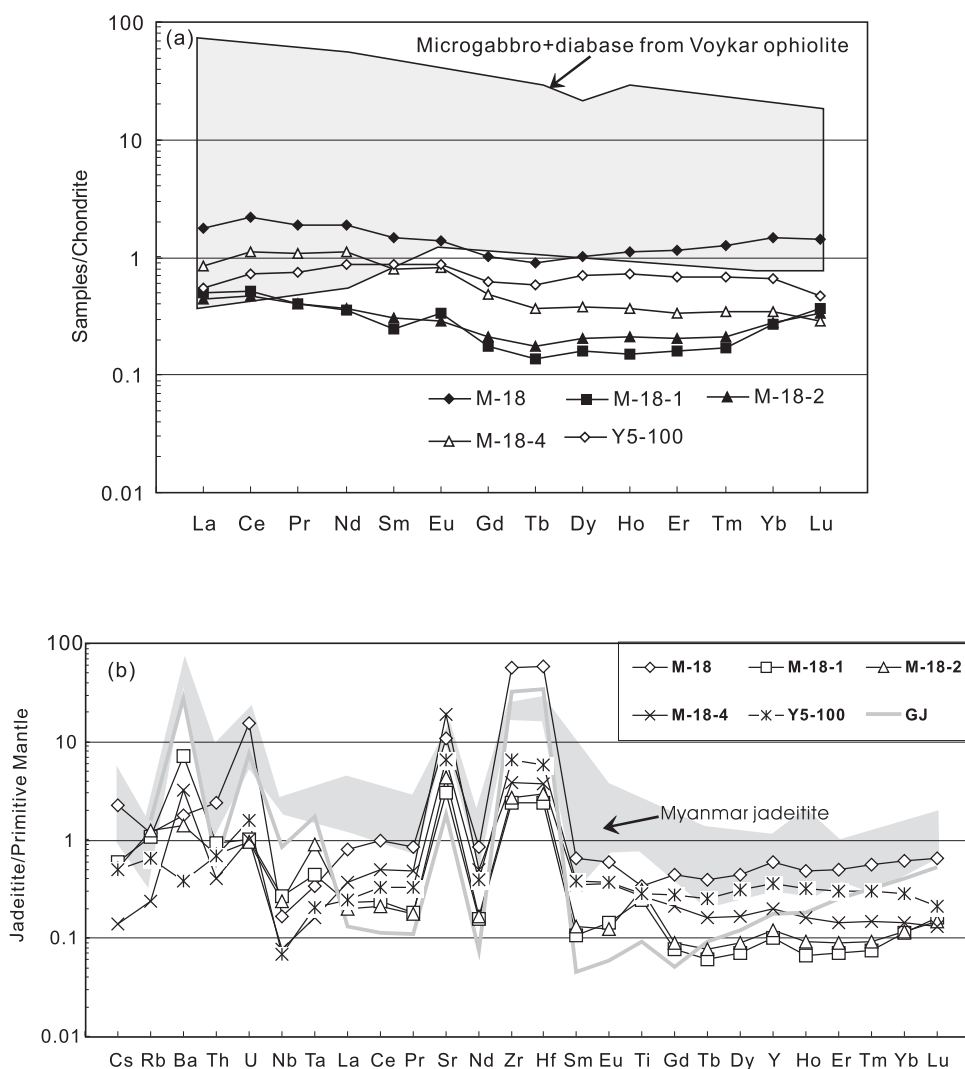

Fig. 4. (a) Chondrite-normalized REE patterns of the jadeitite from Pusyerka, Polar Urals. Chondrite values after Boynton (1984); grey area shows REE patterns of gabbro + diabase from the Voykar ophiolite (data after Saveliev *et al.*, 1999). (b) Primitive mantle - normalized spidergram of the jadeitite. Primitive-mantle values after Sun & McDonough (1989), grey range showing trace element variations of Myanmar jadeitite (data after Shi *et al.*, 2008).

Table 2. Rb-Sr isotopic compositions of jadeitite from SK, Polar Urals, Russia.

No.	Sample	Rb (10^{-6})	Sr (10^{-6})	$^{87}Rb/^{86}Sr$	$^{87}Sr/^{86}Sr$	2σ	$(^{87}Sr/^{86}Sr)t$
1	M-18	0.75	228.6	0.009	0.703480	11	0.703434
2	M-18-1	0.69	64.8	0.031	0.703649	11	0.703489
3	M-18-2	0.79	91.3	0.025	0.703604	11	0.703474
4	M-18-4	0.15	400.4	0.001	0.703525	11	0.703519
5	Y5-100	0.41	136.7	0.009	0.703445	11	0.703400

t = 368 Ma (after Meng *et al.*, 2011)

Table 3. Nd isotopic compositions of jadeitite and ultramafic rocks from SK, Polar Urals, Russia.

Samples		Sm (10^{-6})	Nd (10^{-6})	$^{147}Sm/^{144}Nd$	$^{143}Nd/^{144}Nd$	$T_{DM(Ga)}$	f(Sm/Nd)	$\varepsilon_{Nd}(0)$	$\varepsilon_{Nd}(t)$	Ref.
jadeitite										
M-18		1.14	0.29	0.1534	0.512573	1.46	−0.22	−1.27	0.77	1
M-18-1		0.21	0.05	0.1352	0.512645	0.98	−0.31	0.14	3.02	1
M-18-2		0.22	0.06	0.1596	0.512681	1.32	−0.19	0.84	2.58	1
M-18-4		0.68	0.16	0.1392	0.512636	1.05	−0.29	−0.04	2.66	1
Y5-100		0.53	0.17	0.1964	0.512925	1.97	0.00	5.60	5.61	1
Syum-Keu										
к-30/4	harzburgite	0.059	0.252	0.14313	0.512617	1.15	−0.27	−0.41	2.11	2
г-44	lherzolite	0.086	0.27	0.1935	0.512701	3.36	−0.02	1.23	1.38	2
c-45/1	gabbronorite	0.132	0.304	0.26265	0.513001	−0.47	0.34	7.08	3.98	2

t = 368 Ma (after Meng *et al.*, 2011); 1- this study, analyses performed in Department of earth sciences, National Cheng-kung University, Tainan, Taiwan; 2- Gurskaya & Smelova, 2003.
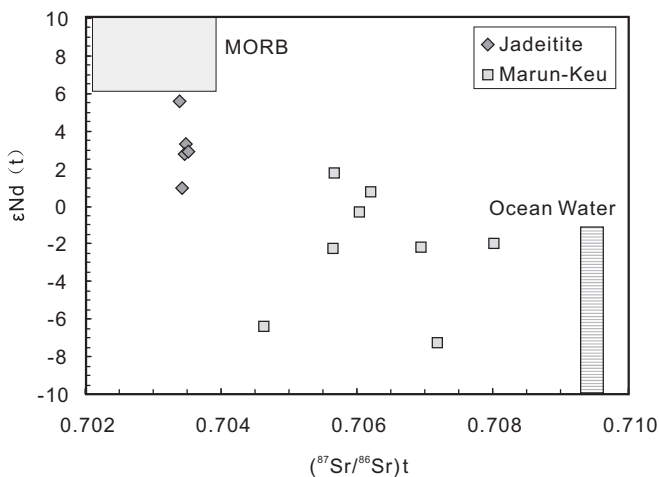

Fig. 5. Sr-Nd isotopic compositions of the jadeitite from Pusyerka in the Polar Urals. Data sources: MORB and ocean water (Zindler & Hart, 1986; DePaolo, 1988), Marun-Keu complex (Glodny *et al.*, 2003, 2004).
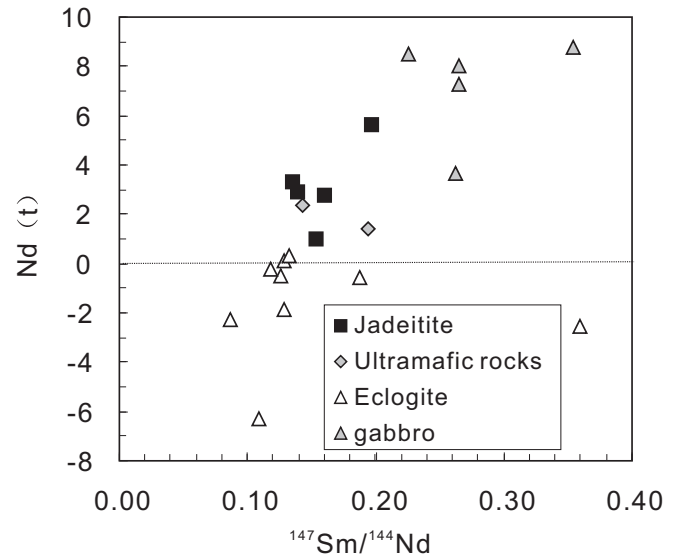

Fig. 6. ^{147}Sm-^{144}Nd isotopic compositions of the jadeitite. Data sources: jadeitite (this study), ultramafic rocks (Gurskaya & Smelova, 2003), eclogite (Shatsky *et al.*, 2000; Glodny *et al.*, 2004; Andreichev *et al.*, 2007), gabbro (Edward & Wasserburg, 1985; Gurskaya & Smelova, 2003).

Fig. 7). Total REE contents vary from 37 to 586 ppm, with heavy REE enrichments represented by (La/Sm)$_{CN}$ of 0.001-1.17, (La/Yb)$_{CN}$ of 0.001-0.01 and (Lu/Gd)$_{CN}$ of 10–83 (Fig. 8). All analyses show positive Ce anomalies with Ce/Ce* ratios of 1.9-99 (Fig. 8), and most zircon grains display negative Eu anomalies, with Eu/Eu* ranging from 0.69 to 0.99 (Table 4, Fig. 8). Hafnium contents of the zircon grains are very high, between 2,126 and 22,522 ppm (Table 4).

4.5. Lu-Hf isotopes of zircon

Thirty-one zircons were measured for their Lu-Hf isotopes, and the results are given in Table 5; thirteen of these analyses yielded SHRIMP ages (Fig. 7, Meng *et al.*, 2011). The $^{176}Hf/^{177}Hf$ ratios of the zircon grains range

Table 4. LA-ICP-MS trace element composition of zircon from jadeitite (sample Y5-100) in SK, Polar Urals, Russia.

Spots	1	2	3	4	5	6	7	8	9	10	11	12	13	14	15	16	17
La	0.1778	0.0357	0.0144	0.0000	0.0040	0.0170	0.0049	0.0021	0.0144	0.0000	0.0579	0.0355	0.0102	2.7180	0.0144	0.0224	0.0745
Ce	6.221	3.315	2.374	0.2464	0.3305	0.5326	6.005	1.498	3.315	3.351	2.178	5.167	1.077	10.53	1.626	1.572	2.751
Pr	0.2045	0.0675	0.0099	0.0091	0.0090	0.0214	0.0458	0.0064	0.0730	0.0000	0.0528	0.0342	0.0194	0.5982	0.0132	0.0082	0.0254
Nd	1.861	1.491	0.3213	0.0921	0.0710	0.5184	1.558	0.1643	1.013	<	0.6183	0.5433	0.3473	3.931	0.2723	0.4175	0.3984
Sm	2.643	3.422	0.7621	0.3064	0.0917	1.505	3.433	0.6315	3.861	<	0.9605	1.634	0.8218	1.462	0.9148	0.6295	0.7727
Eu	1.92	2.218	0.4562	0.2397	0.1	1.072	1.668	0.5148	2.619	1.847	0.5178	1.19	0.6208	0.9922	0.7347	0.7359	0.6204
Gd	15.46	17.35	5.045	1.246	0.6717	7.232	14.03	4.006	20.96	4.325	5.506	12.15	4.718	9.895	6.012	4.384	4.814
Tb	5.002	5.278	1.71	0.2898	0.2351	1.813	3.805	1.376	5.261	1.818	1.846	4.249	1.453	2.976	2.168	1.584	1.554
Dy	60.72	65.56	20.67	3.722	2.938	18.39	39.57	17.6	50.12	21.73	24.48	50.42	17.18	37.58	28.42	19.32	19.11
Ho	21.49	23.76	8.295	1.39	1.193	6.341	12.7	7.235	15.61	8.35	9.117	18.77	6.509	13.3	11.68	7.648	6.851
Er	107.1	119.6	44.86	6.954	7.463	31.71	57.18	37.35	67.45	47.52	45.57	98.31	36.7	67.69	61.82	47.98	34.82
Tm	23.63	26.68	10.25	1.815	2.054	7.085	12.12	8.528	14.48	10.3	10.06	21.14	8.659	15.53	14.08	11.17	7.617
Yb	227.8	258.6	105	16.98	24.99	68.65	112.4	83.71	139	132.5	97.34	192.8	91.75	151.1	159.5	127.9	78.21
Lu	46.86	59.16	23.48	3.653	7.211	14.55	24.28	18.67	27.23	20.18	21.61	40.36	23.42	34.04	35.83	35.03	17.85
Hf	16400	19020	15331	12516	15679	12983	22522	14797	15136	12126	17909	21420	13432	19639	14450	15399	13076
Ta	0.318	0.1542	0.159	0.06007	0.1193	0.1416	1.336	0.09719	0.1198	0.05942	0.1414	0.2379	0.1165	1.939	0.1209	0.2302	0.2066
Pb	2.556	0.3964	0.6105	0.138	0.32	0.1662	8.238	0.5098	1.212	2.276	0.8386	1.656	0.2667	5.171	0.3544	0.7131	0.8721
Th	60.91	7.528	16.7	1.494	1.352	2.216	238.7	13.74	32.31	13.06	17.1	41.57	5.013	201.4	7.728	4.236	20.54
U	200.2	77.37	116.1	22.16	18.4	26.55	390.4	88.91	132.6	70.12	108.1	218.9	39.81	313	60.03	41.2	122.2
∑REE	521.09	586.54	223.25	36.94	47.36	159.44	288.80	181.29	351.01	251.92	219.91	446.80	193.29	352.34	323.09	258.40	175.47
Th/U	0.30	0.10	0.14	0.07	0.07	0.08	0.61	0.15	0.24	0.19	0.16	0.19	0.13	0.64	0.13	0.10	0.17
La_{CN}/Sm_{CN}	0.0423	0.0066	0.0119	0.0000	0.0273	0.0071	0.0009	0.0021	0.0023	<	0.0379	0.0136	0.0078	1.1694	0.0099	0.0224	0.0607
La_{CN}/Yb_{CN}	0.0005	0.0001	0.0001	0.0000	0.0001	0.0002	0.0000	0.0000	0.0001	0.0000	0.0004	0.0001	0.0001	0.0121	0.0001	0.0001	0.0006
Lu_{CN}/Gd_{CN}	23.65	26.60	36.31	22.87	83.75	15.70	13.50	36.36	10.13	36.40	30.62	25.91	38.72	26.84	46.49	62.33	28.93
Eu/Eu*	0.92	0.88	0.71	1.19	1.23	0.99	0.73	0.99	0.89		0.69	0.82	0.96	0.80	0.96	1.35	0.98
Ce/Ce*	7.85	16.26	47.84		13.27	6.73	96.22	99.02	24.64		9.48	35.71	18.41	1.99	28.46	27.87	15.21

Note: <–less than detection limits, Eu/Eu* = $Eu_N/(Sm_N \times Gd_N)^{0.5}$, Ce/Ce* = $Ce_N/(La_N \times Pr_N)^{0.5}$, Analyses performed in National Research Center for Geoanalysis, CAGS, Beijing
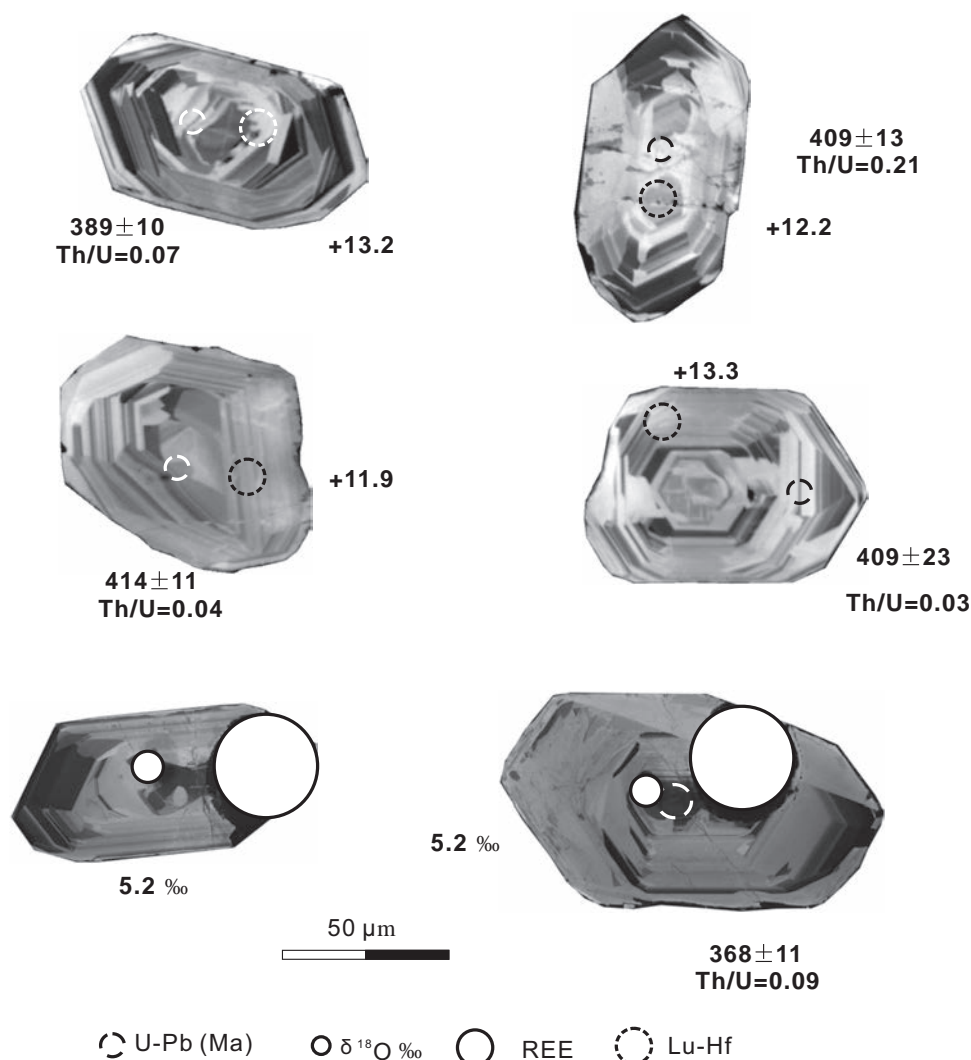
Fig. 7. CL images of zircons from the Pusyerka jadeitite in the Polar Urals, showing ages (Ma), $\delta^{18}O$ values (‰) and ϵHf (t) values for representative zircon grains. Solid circles show U-Pb spots (data from Meng *et al*., 2011); dashed circles show 10 μm diameter ion microprobe oxygen isotope pits; large circles represent laser spots for ϵHf (t) values, large dashed circles show laser spots of trace elements analyses.
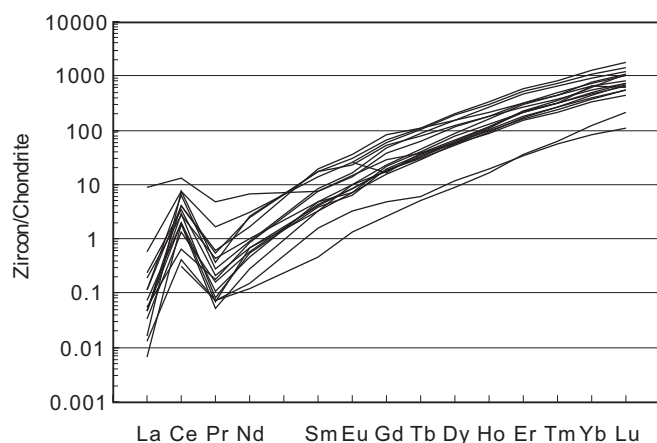

Fig. 8. Chondrite-normalized REE patterns of zircons from jadeitite at Pusyerka, Polar Urals. Chondrite value after Boynton (1984).

from 0.282708 to 0.283017, corresponding to initial epsilon Hf values of +6 to +17 (Fig. 10).

4.6. Oxygen isotopes of zircon

Twenty oxygen isotopic analyses yielded in $\delta^{18}O$ values of 5.03–6.04‰ (Table 6, Fig. 11), with an average of 5.45 ± 0.11‰, consistent with being in equilibrium with mantle-derived melts ($\delta^{18}O$ = 5.3 ± 0.6‰; Valley *et al*., 2005).

5. Discussion

5.1. Fluid composition in an intra-oceanic subduction zone

5.1.1. Genesis of zircon

The origin of zircon in jadeitite has long been debated. Currently, two models are suggested for the zircon

Table 5. Lu-Hf isotopic compositions of zircons from jadeitite (sample Y5-100) in SK, Polar Urals, Russia.

Spots	Age (Ma)	$^{176}Yb/^{177}Hf$	2σ	$^{176}Lu/^{177}Hf$	2σ	$^{176}Hf/^{177}Hf$	2σ	f(Lu/Hf)	εHf(0)	εHf(t)	2σ	T_{DM} (Ga)
1	399	0.018123	0.000686	0.000337	0.000020	0.282860	0.000024	-0.99	3.11	11.77	0.85	0.55
3	372	0.009210	0.000354	0.000219	0.000011	0.282911	0.000026	-0.99	4.92	13.02	0.91	0.47
4	372	0.014997	0.000179	0.000332	0.000007	0.282909	0.000020	-0.99	4.84	12.91	0.71	0.48
5	316	0.009713	0.000201	0.000238	0.000009	0.282870	0.000027	-0.99	3.46	10.34	0.97	0.53
6	399	0.039673	0.001928	0.000962	0.000060	0.282863	0.000026	-0.97	3.22	11.71	0.94	0.55
7	399	0.030511	0.000122	0.000612	0.000003	0.282794	0.000123	-0.98	0.78	9.36	4.36	0.64
8	399	0.021725	0.000110	0.000502	0.000004	0.282785	0.000055	-0.98	0.46	9.07	1.94	0.65
9	399	0.026530	0.000095	0.000573	0.000001	0.282866	0.000026	-0.98	3.32	11.92	0.93	0.54
10	409	0.023153	0.000719	0.000571	0.000025	0.282868	0.000025	-0.98	3.40	12.21	0.87	0.54
11	404	0.018387	0.000911	0.000337	0.000009	0.282927	0.000022	-0.99	5.47	14.24	0.76	0.45
12	404	0.019616	0.000050	0.000411	0.000002	0.282708	0.000070	-0.99	-2.27	6.48	2.47	0.76
13	404	0.038258	0.001211	0.000892	0.000016	0.282954	0.000028	-0.97	6.43	15.05	0.99	0.42
16	414	0.007402	0.000099	0.000168	0.000005	0.282918	0.000022	-0.99	5.18	14.21	0.78	0.46
17	414	0.022955	0.000626	0.000517	0.000016	0.282885	0.000018	-0.98	3.99	12.93	0.64	0.51
18	409	0.008870	0.000200	0.000194	0.000007	0.282895	0.000024	-0.99	4.34	13.26	0.84	0.50
19	404	0.010600	0.000181	0.000226	0.000003	0.282927	0.000017	-0.99	5.47	14.26	0.62	0.45
20	404	0.014646	0.000321	0.000349	0.000014	0.282899	0.000025	-0.99	4.51	13.27	0.89	0.49
21	406	0.022615	0.000575	0.000552	0.000023	0.282884	0.000021	-0.98	3.95	12.70	0.74	0.52
22	404	0.006034	0.000167	0.000144	0.000006	0.282861	0.000019	-1.00	3.13	11.95	0.67	0.54
23	414	0.020768	0.000319	0.000475	0.000014	0.282856	0.000019	-0.99	2.96	11.90	0.66	0.55
24	404	0.017572	0.000100	0.000388	0.000003	0.282879	0.000018	-0.99	3.80	12.55	0.65	0.52
25	404	0.007073	0.000054	0.000181	0.000002	0.282836	0.000026	-0.99	2.25	11.06	0.91	0.58
26	404	0.020378	0.000185	0.000474	0.000005	0.282867	0.000027	-0.99	3.37	12.10	0.95	0.54
27	390	0.008721	0.000272	0.000195	0.000008	0.282904	0.000014	-0.99	4.66	13.16	0.51	0.48
28	404	0.011169	0.001223	0.000260	0.000032	0.282883	0.000019	-0.99	3.93	12.71	0.69	0.51
29	404	0.006505	0.000657	0.000153	0.000016	0.282895	0.000026	-1.00	4.36	13.18	0.93	0.49
30	404	0.021799	0.000584	0.000511	0.000026	0.283017	0.000028	-0.98	8.67	17.39	1.00	0.33
31	404	0.014301	0.000165	0.000344	0.000007	0.282791	0.000022	-0.99	0.69	9.45	0.79	0.64

Analyses performed in Institute of Mineral Resources,CAGS, Beijing

Table 6. *In situ* $\delta^{18}O$ values (‰ VSMOW) by SIMS for zircons from jadeitite (Y5-100) in SK, Polar Urals, Russia.

	$\delta^{18}O$	2σ
Y5-100-1	5.45	0.26
Y5-100-2	5.11	0.28
Y5-100-3	5.62	0.25
Y5-100-4	5.22	0.19
Y5-100-5	5.24	0.35
Y5-100-6	5.75	0.30
Y5-100-7	5.34	0.24
Y5-100-8	5.54	0.33
Y5-100-9	5.39	0.25
Y5-100-10	5.48	0.23
Y5-100-11	5.43	0.27
Y5-100-12	5.49	0.39
Y5-100-13	5.03	0.27
Y5-100-14	5.58	0.19
Y5-100-15	6.04	0.26
Y5-100-16	5.31	0.32
Y5-100-17	5.41	0.38
Y5-100-18	5.43	0.25
Y5-100-19	5.61	0.37
Y5-100-20	5.66	0.35

Note: Analyses performed in institute of Geology and Geophysics, CAS

formation. One suggests a hydrothermal origin (h-type), in which the grains were precipitated directly from Zr-saturated hydrothermal fluids along with jadeitite (*e.g.*, Qiu *et al*., 2009; Yui *et al*., 2010, 2012; Meng *et al*., 2011; Flores *et al*., 2013). The other model suggests a magmatic or igneous origin for the zircons (Shi *et al*., 2008; Fu *et al*., 2010, 2012; Yui *et al*., 2013). These two genetic types of zircon may occur in the same jadeitite, or even the same zircon grain: for example, some zircons have magmatic cores, surrounded by hydrothermal rims (*e.g.*, Fu *et al*., 2010; Mori *et al*., 2011). The two types are distinguished on the basis of internal textures (CL images), mineral or fluid inclusions, compositions (Th/U ratios, REE patterns), U-Pb ages and Hf and oxygen isotopes (*e.g.*, Flores *et al*., 2013).

Most of the zircons from jadeitite sample Y5-100 show clear oscillatory or sector zoning in their CL images (Fig. 7, Meng *et al*., 2011), reflecting an igneous origin. Some of the zircons show clear oscillatory zoning in the core, but have greyish and blurred rims (Fig. 7), similar to zircons from the Osayama jadeitite in SW Japan (Tsujimori *et al*., 2005; Fu *et al*., 2010), which probably reflects modification by hydrothermal fluids.

Thorium and U contents of the zircons obtained by ICP-MS analysis vary from 2 to 239 ppm and 41 to 390 ppm, respectively, producing a wide range of Th/U ratios (0.07-0.64, Table 4). Similar analyses using the SHRIMP method produced Th and U concentrations of 2 to 12 ppm, and 48 to 158 ppm, respectively, yielding Th/U ratios from 0.03 to 0.21, and mostly less than 0.1 (Meng *et al*., 2011). Although Th/U ratios alone cannot confirm the origin of individual zircon grains (Harley *et al*., 2007), it is generally accepted that hydrothermal
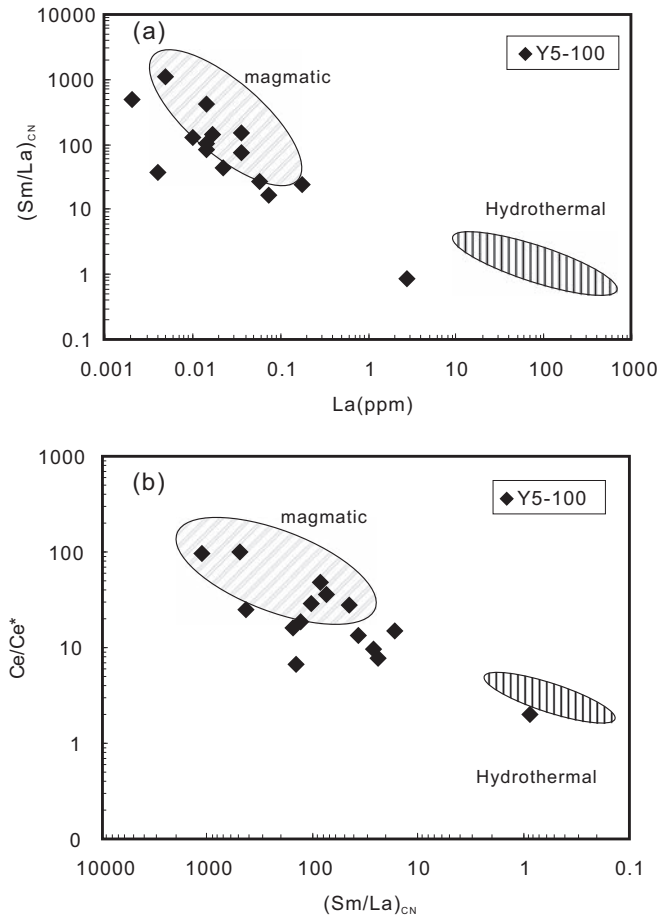

Fig. 9. Discrimination plots of (a) $(Sm/La)_{CN}$ *vs*. La (ppm); (b) Ce/Ce* *vs*. $(Sm/La)_{CN}$ for zircons from the Polar Urals jadeitite (sample Y5-100). The two outlined areas are defined by magmatic and hydrothermal zircon from the Boggy Plain Zoned Pluton (after Hoskin, 2005). Chondrite values after Boynton (1984).
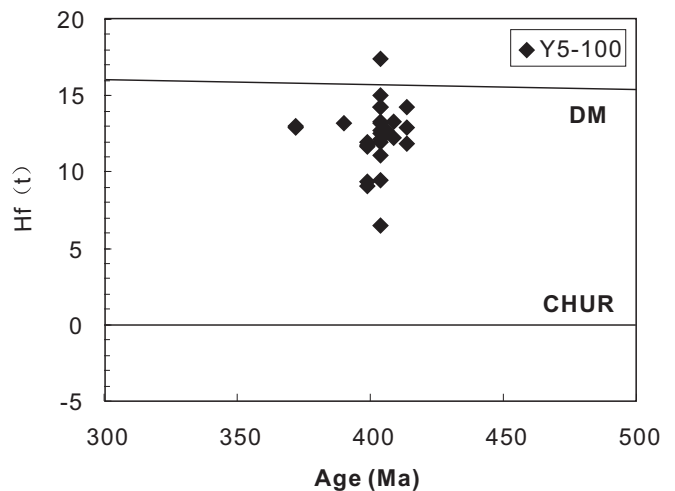

Fig.10. εHf(t) *versus in situ* SHRIMP U-Pb ages of zircons from jadeitite at Pusyerka in the Polar Urals. The age data are from Meng *et al*. (2011)
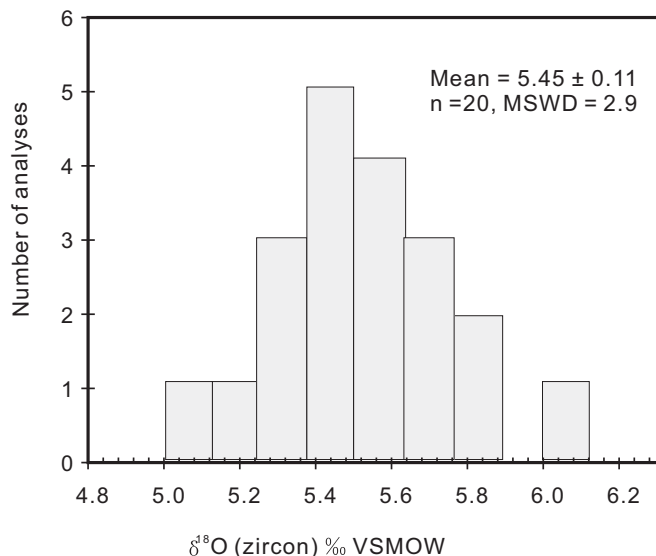
Fig.11. Histograms of ion microprobe δ^{18}O values of zircons from the jadeitite at Pusyerka in the Polar Urals. For data sources see Table 6.

zircons have very low Th/U ratios, mostly less than 0.1 (Flores *et al.*, 2013; Yui *et al.*, 2013). Hence, our zircons may reflect both hydrothermal and igneous processes.

Most of the zircons show weak negative Eu anomalies (δEu = 0.69-0.99, Table 4; Fig. 8), but three show positive Eu anomalies (1.19, 1.23 and 1.35), which are similar to those of hydrothermal grains in jadeitites in Myanmar and Guatemala (Flores *et al.*, 2013; Yui *et al.*, 2013). Zircons from oceanic gabbros, plagiogranites and ophiolites display obvious negative Eu anomalies (Grimes *et al.*, 2007, 2009). Yui *et al.* (2010) suggested that positive or negative Eu anomalies of zircons reflect the presence or absence, respectively, of plagioclase in rocks through which the hydrothermal fluids migrated.

On plots of $(Sm/La)_{CN}$ *vs.* La (ppm) and Ce/Ce* *vs.* $(Sm/La)_{CN}$ (Fig. 9), most of the zircons of jadeitite sample Y5-100 fall in the magmatic field.

Moreover, the zircons have high positive ϵHf(t) values (+6 to +17, Table 5, Fig. 10), similar to those of igneous or hydrothermal zircons in jadeitite from Myanmar (+11 to +20), Japan (+10 to +15), Guatemala (+11 to +13) and Greece (+10 to +24) (Qiu *et al.*, 2009; Shi *et al.*, 2009; Fu *et al.*, 2012; Yui *et al.*, 2012). These values are consistent with those of depleted mantle and young oceanic crust, suggesting that the protoliths or fluids from which the jadeitite was formed were related to subducted oceanic crust (Qiu *et al.*, 2009; Shi *et al.*, 2009; Yui *et al.*, 2012). The ϵHf(t) values of the zircon in the Syum-Keu jadeitite approach those of zircons from plagiogranite in the Oytag ophiolitic suite, northwest China (ϵHf(t) +13 to +20, Jiang *et al.*, 2008), suggesting they are related to depleted-mantle-derived magma (Fu *et al.*, 2012).

The average oxygen isotopic composition of the SK zircons (5.45 ± 0.11‰; Table 6, Fig. 11) is similar to that of zircons in the the Syros jadeitite, Greece (δ^{18}O 5.2 ±0.5‰, Fu *et al.*, 2010) and in peridotite, plagiogranite and gabbro in mid-ocean ridges and ophiolites (Mattey *et al.*, 1994; Cavosie *et al.*, 2009; Grimes *et al.*, 2011, 2013). These data point to an igneous origin for the SK zircons and suggest that they are igneous grains inherited from precursor rocks (*e.g.*, Fu *et al.*, 2010). In contrast, zircons crystallized from fluids show relatively lower oxygen isotopic values, such as the hydrothermal zircons from jadeitite in Osayama, SW Japan (δ^{18}O = 3.2–4.5‰; Fu *et al.*, 2010).

In summary, Th, U, and Eu concentrations, and Th/U ratios of the zircons from the SK jadeitite Y5-100 display hydrothermal features, and the La, Sm, Ce and Hf-O isotopic compositions reflect intense igneous signals. Therefore, we infer that the zircons of the jadeitite may have been acquired from precursor igneous rocks and reworked by Na–Al–Si-rich fluids, which were released from a subduction zone. The youngest age of the zircons in the jadeitite is 368 ± 11 Ma (Meng *et al.*, 2011), which is close to the formation age of the 360–355 Ma MK eclogite (Shatsky *et al.*, 2000; Glodny *et al.*, 2003, 2004), implying that the zircon-bearing jadeitite might have been modified by fluids related to this subduction zone.

The igneous zircons of the jadeitite may have had two sources: (1) *in situ* zircons inherited from plagiogranites and gabbros, which were partially replaced by Na–Al–Si-rich fluids and transformed into jadeitite (R-type), with zircons being preserved (Shi *et al.*, 2008, 2009; Yui *et al.*, 2013); because the formation temperature and pressure conditions of plagiogranite and gabbro are quite different from those of jadeitite, these zircons could not have formed *in situ*; (2) xenocrystal zircons, which were picked up and transported by Na–Al–Si-rich fluids passing through the igneous rocks and then preserved in newly formed jadeitite (P-type) (Tsujimori & Harlow, 2012). This scenario is quite similar to the inherited zircons in quartz veins crossing eclogite, where the zircons experienced short-distance physical transportation (Sheng *et al.*, 2012), as indicated by their Hf-O isotope features.

Considering that the jadeitite occurs in serpentinized peridotite (Fig. 2a, b), and that zircons in the jadeitite have relatively uniform Hf-O isotope compositions (Figs 10 and 11), we estimate that fluids containing zircon xenocrysts rose from a subduction zone into an overlying mantle wedge (Morishita *et al.*, 2007; Bebout & Penniston-Dorland, 2015), where the jadeitite was precipitated. Thus, zircons were incorporated in the jadeitite, which crystallized at temperatures less than 450°C (*e.g.*, Harlow & Sorensen, 2005), thereby preserving the Hf-O isotope features of the zircon (Figs 10 and 11).

5.1.2. *Source of the Na-Al-Si fluids*

Several studies have argued that the major elements of R-type jadeitites can be derived from precursor rocks, such as plagiogranite, metagabbro and eclogite (Dobretsov &

Ponomareva, 1965; Harlow & Sorensen, 2005; Yui *et al.*, 2010; Tsujimori & Harlow, 2012; Wang *et al.*, 2012), whereas others propose that the Na-, Al- and Si-rich fluids can be produced only by dewatering of sediments (Harlow & Sorensen, 2005). However, experiments have shown that high-pressure fluids can be enriched in Na, Ca, Al and Si (*e.g.*, Manning, 1998, 2004). On the basis of their occurrence (Fig. 2b, d), fluid inclusions and oscillatory zoning, we have classified the jadeitites of the SK complex as P-type (Meng *et al.*, 2011). Although the zircon inclusions in the analysed jadeitite are of igneous origin, their rims show evidence of precipitation from fluids, consistent with the P-type origin of the jadeitite (Tsujimori & Harlow, 2012). The igneous zircons are therefore xenocrysts picked up by the jadeitite-forming fluids. We infer that the jadeitite-forming fluids obtained their Na-Al-Si components while migrating through the igneous protoliths (Harlow & Sorensen, 2005). The jadeitite was then precipitated when these fluids interacted with peridotite in the overlying mantle wedge. This interpretation is supported by the fact that the jadeitites have higher contents of Na_2O and Al_2O_3 than those of the eclogite, metagranite, and metasediment in the MK complex, as well as the gabbro and diabase of the Voykar ophiolite (Fig. 3a, b). Our data show that these igneous and metaigneous rocks were not direct protoliths of the jadeitite, but instead were the sources of the major constituents in the jadeitite-forming fluids from which jadeitites crystallized, thus providing further support for their P-type origin.

5.1.3. Source of the trace elements

Chondrite-normalized REE patterns of the jadeitites (Fig. 4a) show that the LREE are slightly enriched relative to the HREE for all samples. The pattern of sample M-18 is similar to those of microgabbro and diabase from the Voykar ophiolite, which formed in a split-arc or back-arc basin, and represents the Polar Urals oceanic crust (Edwards & Wasserburg, 1985; Saveliev *et al.*, 1999). Slight positive Eu anomalies (δEu = 1.12-1.60) of the jadeitite suggest that they were inherited from plagioclase of the precursor source rocks (Yui *et al.*, 2010). These patterns resemble those of omphacite from the Itoigawa–Ohmi district, Japan (Morishita *et al.*, 2007) and Myanmar jadeitite (Shi *et al.*, 2008), as well as Guatemala jadeitite (Yui *et al.*, 2010). The above facts support our interpretation that jadeitite-forming fluids were either derived from the oceanic crust or reacted with it.

The spidergrams of the jadeitites (Fig. 4b) are strikingly similar to those of the Myanmar jadeitite (Shi *et al.*, 2008). The jadeitites have high Ba and Sr contents, about 1.2-7.3 times and 3–19 times higher than primitive mantle values, respectively (Table 1, Fig. 4b). Such enrichment of Ba and Sr is commonly interpreted to be derived from abyssal sediments (Harlow, 1994; Morishita, 2005; Shi *et al.*, 2008, 2010, 2012), so that the jadeitite-forming fluids were probably infused with fluids and other material derived from abyssal sediments. However, modelling of Li isotopic compositions

of Guatemala jadeitite showed that only about 5–10 % of the Li in the fluids was derived from sediment, with the remainder coming from altered oceanic crust (Simons *et al.*, 2010). Apparently, the contribution of sediment to jadeitite formation is minor. In addition, the results of experiments demonstrate that serpentinites contain significant amounts of fluid-mobile elements, such as B, Cs, As and Ba, which can be incorporated into mantle rocks during seafloor alteration. When such serpentinites are dehydrated in subduction zones, the mobile elements will be strongly enriched in the released fluids (Ulmer & Trommsdorff, 1995; Scambelluri *et al.*, 2004; Tenthorey & Hermann, 2004; Spandler *et al.*, 2009, 2011; Deschamps *et al.*, 2013). The Sr and Ba in the jadeitites were likely derived from plagioclase in igneous rocks through which the fluids passed (Yui *et al.*, 2010).

Zirconium and Hf concentrations of the jadeitite vary from 27 to 637 ppm and 1 to18 ppm, about 2–57 times and 2–58 times higher than primitive mantle, respectively (Table 1). Thus, zircon occurring as inclusions in jadeite, or as interstitial phases between jadeite crystals, is the predominant Zr- and Hf-bearing phase in these rocks (Fig. 2c). On the basis of the La, Sm, Ce and Hf-O isotopic compositions of the zircons, we consider that they are xenocrystals (Figs 9–11), because zircons are common in plagiogranite and evolved gabbro from modern oceans (*e.g.*, Grimes *et al.*, 2009) and from ophiolites (Rubatto *et al.*, 1998; Liati *et al.*, 2004; Kaczmarek *et al.*, 2008). Although zircon is rare in ultramafic rocks, small amounts of this mineral have been found in podiform chromitites and peridotites of ophiolites (Grieco *et al.*, 2001; Zaccarini *et al.*, 2004; Savelieva *et al.*, 2006, 2013; Yamamoto *et al.*, 2013; Robinson *et al.*, 2015), suggesting that magmatic or metasomatic events occurred in the upper mantle (Grieco *et al.*, 2001; Savelieva *et al.*, 2006), or that the mantle peridotite was contaminated by the crustal materials (Yamamoto *et al.*, 2013; Robinson *et al.*, 2015). Most of the zircons from jadeitites in Myanmar, Japan, and Greece are igneous in origin, but are interpreted as xenocrysts inherited from precursor rocks (Shi *et al.*, 2008; Fu *et al.*, 2010, 2012; Mori *et al.*, 2011; Yui *et al.*, 2013). On the other hand, some hydrothermal zircon appears to have crystallized from Zr and Hf-rich hydrothermal fluids (Tsujimori *et al.*, 2005; Qiu *et al.*, 2009; Yui *et al.*, 2010; Flores *et al.*, 2013). Zirconium and Hf enrichment in the fluid indicates that these elements can be transferred in subduction zones by alkalic fluids (Dubinska *et al.*, 2004; Sorensen *et al.*, 2006, 2010; Morishita *et al.*, 2007; Shi *et al.*, 2008; Simons *et al.*, 2010; Yui *et al.*, 2010, 2012). Alkaline fluids produced by dehydration of serpentinite can dissolve zircon from the ultramafic rocks and enrich the fluids in Zr and Hf (Dubinska *et al.*, 2004; Manning, 2004; Tsujimori *et al.*, 2005; Li *et al.*, 2010b; Sorensen *et al.*, 2010; Yui *et al.*, 2010). However, *in situ* measurement of the SK jadeite shows that Zr and Hf contents (6–104 ppm and 0.2–3 ppm, respectively) (Table 7, Fig. 12) are very low, similar

Table 7. *In situ* trace element (ppm) analyses of jadeite from jadeitite sample (sample Y5-100) in SK, Polar Urals, Russia.

Sample	Y5-100																		
Spots	1	2	3	4	5	6	7	8	9	10	11	12	13	14	15	16	17	18	19
La	0.02	0.08	0.35	0.11	0.07	0.00	0.02	0.02	0.09	0.00	0.03	0.01	0.00	0.02	0.02	0.01	0.01	0.02	0.08
Ce	0.12	0.18	0.74	0.29	0.26	0.04	0.03	0.02	0.27	0.02	0.19	0.03	0.03	0.07	0.07	0.05	0.11	0.04	0.22
Pr	0.05	0.05	0.15	0.06	0.04	0.01	0.00	0.02	0.07	0.02	0.03	0.02	0.02	0.01	0.03	0.02	0.05	0.01	0.07
Nd	0.31	0.19	0.35	0.18	0.26	0.15	0.00	0.12	0.27	0.11	0.60	0.18	0.07	0.13	0.03	0.03	0.13	0.17	0.13
Sm	0.00	0.09	0.14	0.10	0.07	0.06	0.08	0.08	0.07	0.00	0.10	0.00	0.00	0.00	0.00	0.09	0.08	0.00	0.00
Eu	0.06	0.03	0.06	0.00	0.05	0.00	0.02	0.06	0.06	0.02	0.00	0.00	0.03	0.07	0.02	0.00	0.00	0.03	0.08
Gd	0.25	0.15	0.08	0.08	0.17	0.04	0.08	0.16	0.11	0.09	0.13	0.11	0.06	0.00	0.12	0.02	0.16	0.05	0.19
Tb	0.01	0.01	0.02	0.02	0.03	0.01	0.00	0.02	0.02	0.00	0.02	0.01	0.01	0.00	0.03	0.01	0.01	0.00	0.02
Dy	0.11	0.04	0.08	0.06	0.10	0.06	0.02	0.09	0.13	0.01	0.17	0.05	0.01	0.08	0.19	0.10	0.06	0.03	0.02
Ho	0.02	0.00	0.02	0.03	0.02	0.02	0.00	0.01	0.03	0.00	0.02	0.01	0.01	0.00	0.02	0.00	0.02	0.01	0.02
Er	0.01	0.09	0.09	0.03	0.09	0.04	0.05	0.03	0.08	0.01	0.11	0.07	0.07	0.06	0.10	0.06	0.08	0.08	0.05
Tm	0.01	0.01	0.03	0.02	0.01	0.02	0.01	0.01	0.03	0.02	0.02	0.01	0.02	0.01	0.03	0.01	0.01	0.02	0.01
Yb	0.09	0.13	0.06	0.03	0.08	0.11	0.01	0.05	0.06	0.03	0.13	0.08	0.00	0.08	0.05	0.07	0.11	0.03	0.21
Lu	0.01	0.00	0.01	0.01	0.01	0.01	0.01	0.02	0.00	0.00	0.01	0.01	0.02	0.01	0.01	0.01	0.01	0.01	0.01
Y	0.64	0.35	0.43	0.62	0.63	0.54	0.25	0.56	0.52	0.30	0.78	0.54	0.43	0.48	0.64	0.27	0.33	0.24	0.34
Li	33.68	47.57	47.75	31.83	28.14	30.21	26.67	25.59	29.57	18.56	29.08	24.51	25.33	29.36	29.30	33.72	36.75	34.96	35.47
Be	0.00	0.00	0.00	0.00	0.00	0.00	0.00	4.44	0.00	1.48	0.00	0.00	7.83	0.00	0.00	0.34	4.73	0.00	0.01
B	0.70	18.50	6.32	0.94	5.94	0.19	2.48	1.45	5.45	0.35	1.77	0.88	0.68	0.96	1.96	1.90	6.12	2.13	2.00
Sc	0.46	0.72	0.59	0.71	0.77	0.66	0.68	0.85	0.77	0.63	0.38	0.89	0.57	0.80	0.53	0.50	0.29	0.85	0.64
V	27.86	19.45	6.11	10.68	40.03	19.49	15.21	14.40	11.44	9.12	17.30	10.99	21.28	11.59	8.48	10.30	10.37	7.56	7.14
Cr	23.43	0.36	0.00	0.00	17.28	2.82	0.00	0.24	20.22	0.00	3.56	0.00	1.60	0.40	0.04	1.02	0.00	0.00	3.82
Co	2.06	2.27	1.66	2.83	1.75	2.46	2.37	3.18	1.90	2.37	3.06	2.92	2.47	2.38	2.40	1.85	2.06	1.90	2.09
Cu	0.00	0.00	2.66	5.31	0.00	0.22	0.53	0.00	0.71	0.21	0.00	1.17	0.48	0.00	0.00	2.66	0.00	0.00	24.49
Zn	3.77	5.28	5.90	5.54	4.36	4.40	4.76	6.34	3.74	3.76	5.47	7.43	5.85	5.97	3.39	6.92	6.09	7.41	3.91
Ga	13.80	18.13	22.18	18.17	13.92	17.68	17.83	19.07	14.29	16.70	19.04	19.50	19.00	17.40	19.48	19.16	17.82	17.19	15.34
Ge	1.39	0.85	0.03	0.00	0.00	0.05	0.00	0.09	0.78	1.48	0.14	0.00	0.87	0.00	0.32	0.00	1.14	0.00	0.64
As	0.24	0.32	0.78	0.65	0.14	0.00	0.83	0.62	0.60	0.00	0.02	0.59	0.56	0.00	0.48	0.35	0.34	0.46	0.06
Rb	0.08	0.09	0.04	0.02	0.00	0.00	0.00	0.00	0.12	0.00	0.00	0.00	0.00	0.00	0.00	0.00	0.04	0.00	0.14
Sr	46.42	58.61	36.88	62.49	51.07	40.05	17.10	20.36	42.17	21.20	83.98	19.13	26.00	24.11	21.60	22.90	25.15	18.23	42.92
Ba	0.06	0.57	0.47	0.25	0.61	0.19	0.71	0.64	0.64	0.13	0.74	0.23	0.00	0.36	0.61	0.00	0.07	0.00	0.86
Mo	0.07	0.00	0.23	0.00	0.00	0.00	0.01	0.05	0.03	0.00	0.01	0.00	0.00	0.11	0.00	0.36	0.12	0.08	0.00
Ag	0.00	0.00	0.03	0.00	0.18	0.14	0.00	0.17	0.00	0.67	0.00	0.04	0.01	0.00	0.07	0.00	0.00	0.30	0.53
Cd	0.00	0.06	0.00	0.23	0.00	0.37	0.18	0.33	0.00	0.00	0.00	0.31	0.65	0.00	0.00	0.39	0.23	0.00	0.22
In	0.00	0.03	0.03	0.00	0.02	0.00	0.00	0.00	0.00	0.01	0.00	0.04	0.00	0.00	0.06	0.01	0.00	0.00	0.00
Sn	0.31	0.53	1.50	0.44	0.00	0.75	0.00	1.30	0.45	0.00	0.39	0.95	0.30	0.00	0.54	0.48	0.00	0.00	0.00
Sb	0.03	0.04	0.00	0.03	0.05	0.01	0.07	0.04	0.00	0.03	0.00	0.03	0.00	0.00	0.02	0.00	0.00	0.00	0.00
Cs	0.00	0.00	0.00	0.00	0.01	0.00	0.05	0.01	0.06	0.00	0.00	0.00	0.00	0.00	0.00	0.00	0.00	0.00	0.03
Zr	12.08	10.78	10.60	46.85	51.56	10.90	6.10	104.84	16.06	15.12	19.02	77.28	16.16	32.19	54.08	30.34	11.18	24.82	18.08
Hf	0.41	0.34	0.48	1.72	1.60	0.34	0.29	3.47	0.39	0.55	0.83	2.44	0.32	0.79	1.67	0.72	0.15	0.46	0.38
Nb	0.01	0.01	0.03	0.01	0.08	0.01	0.01	0.02	0.01	0.02	0.00	0.01	0.00	0.01	0.02	0.00	0.04	0.04	0.01
Ta	0.00	0.01	0.00	0.01	0.01	0.01	0.00	0.03	0.00	0.00	0.00	0.03	0.00	0.00	0.00	0.01	0.01	0.01	0.00
W	0.02	0.02	0.06	0.01	0.06	0.00	0.09	0.10	0.00	0.03	0.03	0.00	0.00	0.02	0.13	0.00	0.00	0.00	0.05

(*continued*)

Table 7. (Continued).

Sample	Y5-100																		
Spots	1	2	3	4	5	6	7	8	9	10	11	12	13	14	15	16	17	18	19
Pt	0.01	0.00	0.00	0.00	0.02	0.04	0.01	0.13	0.00	0.04	0.00	0.00	0.04	0.00	0.03	0.00	0.07	0.00	0.04
Au	0.06	0.00	0.00	0.05	0.06	0.03	0.00	0.00	0.00	0.00	0.00	0.09	0.00	0.06	0.00	0.00	0.00	0.01	0.00
Tl	0.00	0.00	0.00	0.00	0.00	0.00	0.00	0.00	0.00	0.00	0.00	0.00	0.00	0.00	0.01	0.00	0.00	0.00	0.00
Pb	0.00	0.03	0.00	0.01	0.03	0.05	0.03	0.00	0.03	0.05	0.00	0.00	0.04	0.00	0.05	0.15	0.03	0.00	7.82
Bi	0.00	0.00	0.00	0.00	0.00	0.00	0.00	0.00	0.01	0.00	0.00	0.00	0.01	0.00	0.01	0.01	0.00	0.00	0.00
Th	0.00	0.00	0.03	0.01	0.02	0.00	0.00	0.00	0.00	0.00	0.00	0.00	0.00	0.00	0.00	0.01	0.00	0.01	0.01
U	0.00	0.01	0.01	0.01	0.01	0.00	0.00	0.00	0.01	0.00	0.00	0.00	0.00	0.00	0.00	0.00	0.00	0.00	0.01
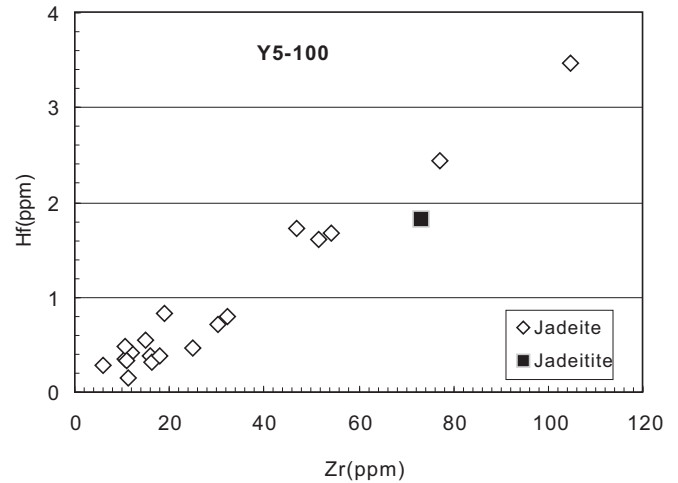
Fig.12. Plot of Zr and Hf content for jadeite and jadeitite (sampleY5-100) from Pusyerka in the Polar Urals.

to those of jadeitites in Myanmar (0–1 and 0.04 ppm) and Guatemala (0–92 and 0–3 ppm) (Sorensen et al., 2006). These data indicate that the Zr and Hf in the SK jadeitite were not dissolved in the jadeitite-forming fluids, but were carried by xenocrystic zircon.

5.1.4. Sr-Nd isotopic constraints

Jadeitites from Guatemala, Japan and Myanmar contain Ba-rich minerals, which suggests that the jadeitite-forming fluids came from subducted sediment (Harlow, 1994; Morishita, 2005; Shi et al., 2010, 2012). Lithium isotopes reveal the presence of minor fluids derived from sediment in subduction zones during jadeitite formation (e.g., Simons et al., 2010). Additionally, oceanic sediments affected by seawater usually have somewhat elevated $^{87}Sr/^{86}Sr$ ratios (>0.705, Zindler & Hart, 1986). However, jadeitite of the SK complex lacks Ba-rich minerals, and $^{87}Sr/^{86}Sr$ ratios of the jadeitites vary from 0.7033 to 0.7034 (Table 2, Fig. 5), close to those of MORB and of gabbro from the Voykar ophiolite (Edwards & Wasserburg, 1985; Zindler & Hart, 1986; DePaolo, 1988; Sharma et al., 1995), implying that the jadeitite-forming fluids were in equilibrium with MORB-type rocks. Seawater has a much higher $^{87}Sr/^{86}Sr$ ratio (0.7091, DePaolo, 1988) than the SK jadeitites, so it cannot be the source for the jadeitite-forming fluids. The $^{87}Sr/^{86}Sr$ ratios of the jadeitites are also different from those of eclogites of the MK complex (0.7055-0.7112, Andreichev, 2003; Glodny et al., 2003). These observations support our interpretation that the Na-Al-Si-rich fluid, from which the jadeitites formed, was derived from a subducted oceanic slab with little or no sediment.

The SK jadeitites have positive εNd(t) values (+1 to +6) (Table 3, Fig. 6, t = 368 Ma, Meng et al., 2011). In contrast, oceanic sediments have lower εNd values (– 15 to –5, DePaolo, 1988); likewise, the MK eclogites have mainly negative εNd(t) values (+0.3 to –6.3; Shatsky et al., 2000; Glodny et al., 2004; Andreichev et al., 2007), whereas the microgabbro and diabase of the

Voykar ophiolite have positive εNd(t) values (+7.3 to +9.8; Edwards & Wasserburg, 1985; Sharma *et al.*, 1995). The εNd(t) values of the SK jadeitite are significantly different from all of these possible sources (Fig. 6), and their heterogeneous compositions (Table 3) suggest mixing from several sources. We propose that the jadeitites were derived mainly from subducted oceanic crust (such as gabbro and plagiogranite), with a minor input from the overlying sediments, which have negative εNd(t) values.

The SK jadeitites have Sr and Nd isotopic compositions that differ significantly from oceanic sediments (Tables 2 and 3), and could not have been derived primarily from such a source. However, minor input from sedimentary fluids cannot be excluded for those samples with relatively low positive εNd(t) values (Table 3). Mixing of fluids from different sources is supported by the oscillatory zoning observed in the SK jadeite grains (Meng *et al.*, 2011), a feature also reported from jadeitite of Myanmar, Guatemala, Japan and Cuba (Sorensen *et al.*, 2006; García-Casco *et al.*, 2009; Shi *et al.*, 2009; Cárdenas-Párraga *et al.*, 2012). Thus, we conclude that igneous rocks provided most of the material for the SK jadeitite formation, but that this material was modified by fluid/melt processes in a subduction zone.

5.2. Formation of the jadeitites

It has been proposed that the SK complex is a SSZ-type ophiolite (Shmelev, 2011). Initial subduction of the oceanic lithosphere may have occurred at 368 ± 11 Ma (Meng *et al.*, 2011). Basalt, gabbro and serpentinite in the subducted oceanic lithosphere underwent high-pressure metamorphism releasing Na–Al–Si-rich fluids (*e.g.*, Peacock, 1990; Li *et al.*, 2004; Gao *et al.*, 2007; Morishita *et al.*, 2007; Spandler *et al.*, 2011). On the basis of our geochemical data for the jadeitites from the Polar Urals, we infer that the Na–Al–Si-rich fluids, which produced the jadeitites, were derived primarily from subducting oceanic lithosphere. This fluid migrated from the subducted lithosphere into the overlying mantle wedge, and then infiltrated into fractures in the peridotite, resulting in serpentinization and jadeitite precipitation (Harlow & Sorensen, 2005; Morishita *et al.*, 2007; Meng *et al.*, 2011).

6. Conclusions

Major element (Na, Al and Si) and trace element (Sr-Ba and Zr-Hf) enrichment and depleted mantle-like Sr-Nd isotopic compositions in the jadeitite from the Polar Urals suggest that the fluids, from which the jadeitite were precipitated, were derived mainly from subducted oceanic igneous rocks. Contributions from sediments in the subduction zone were minor. Zircons in the jadeitite show both "igneous" and "hydrothermal" features, which suggest that magmatic zircons were picked up from the subducted igneous rocks and transported by fluids in the suprasubduction-zone mantle wedge.

References

Andreichev, V.L. (2003): K-Ar, Rb-Sr, Sm-Nd and Pb-Pb isotopic geochronology system in Marun-Keu eclogite block (Polar Ural). Geoprint, Syktyvkar. 25 p. (in Russian).

— (2004): Isotopic geochronology of ultramafic-mafic and granitic rocks in the eastern slope, Polar Ural, Russia. Geoprint, Syktyvkar. 43 p. (in Russian).

Andreichev, V.L., Ronkin, Yu.L., Serov, P.A., Lepikhina, O.P., Litvinenko, A.F. (2007): New data on the Precambrian age of Marunkeu eclogites (Polar Urals). *Dokl. Earth Sci.*, **413A**, 347–350.

Bebout, G.E. & Penniston-Dorland, S. (2015): Fluid and mass transfer at subduction interfaces - the field metamorphic record. *Lithos*, **240–243**, 228–258. doi:10.1016/j.lithos.2015.10.007

Black, L.P., Kamo, S.L., Allen, C.M., Davis, D.W., Aleinikoff, J.N., Valley, J.W., Mundil, R., Campbell, I.H., Korsch, R.J., Williams, I.S., Foudoulis, C. (2004): Improved Pb- 206/U-238 microprobe geochronology by the monitoring of a trace-element-related matrix effect; SHRIMP, ID-TIMS, ELA-ICP-MS and oxygen isotope documentation for a series of zircon standards. *Chem. Geol.*, **205**, 115–140.

Blichert-Toft, J. & Albarede, F. (1997): The Lu-Hf isotope geochemistry of chondrites and the evolution of the mantle–crust system. *Earth Planet. Sci. Lett.*, **148**, 243–258.

Boynton, W.V. (1984): Geochemistry of the rare earth elements: meteorite studies. *in* "Rare earth element geochemistry", P. Henderson, ed. Elsevier, 63–114.

Cardenas-Parraga, J., Garcia-Casco, A., Harlow, G.E., Blanco-Quintero, I.F., Rojas Agramonte, Y., Kröner, A. (2012): Hydrothermal origin and age of jadeitites from Sierra del Convento Melange (Eastern Cuba). *Eur. J. Mineral.*, **24**, 313–331.

Cavosie, A.J., Kita, N.T., Valley, J.W. (2009): Primitive oxygen-isotope ratio recorded in magmatic zircon from the Mid-Atlantic Ridge. *Am. Mineral.*, **94**, 926–934.

Compagnoni, R., Rolfo, F., Castelli, D. (2012): Jadeitite from the Monviso meta-ophiolite, western Alps: occurrence and genesis. *Eur. J. Mineral.*, **24**, 333–343.

DePaolo, D.J. (1988): Neodymium isotope geochemistry-an introduction. Springer-Verlag Berlin Heidelberg, 1–181 p.

Deschamps, F., Godard, M., Guillot, S., Hattori, K. (2013): Geochemistry of subduction zone serpentinites: A review. *Lithos*, **178**, 96–127.

Dobretsov, N.L. (1991): Blueschists and eclogites: a possible plate tectonic mechanism for their emplacement from the upper mantle. *Tectonophysics*, **186**, 253–268.

Dobretsov, N.L. & Ponomareva, L.G. (1965): Comparative characteristics of jadeite and associated rocks from Polar Ural and Near-Balkhash Region: USSR Academy of Sciences (Siberian Branch). *Proc. Inst. Geol. Geophys.*, **31**, 178–243.

Dobretsov, N.L. & Sobolev, N.V. (1984): Glaucophane schists and eclogites in the folded systems of Northern Asia. *Ofioliti*, **9**, 401–424.

Dubinska, E., Bylina, P., Kozlowski, A., Dorr, W., Nejbert, K., Schastok, J., Kulicki, C. (2004): U-Pb dating of serpentinization: hydrothermal zircon from a metasomatic rodingite shell (Sudetic ophiolite, SW Poland). *Chem. Geol.*, **203**, 183–203.

Edward, R.L. & Wasserburg, G.J. (1985): The age and emplacement of obducted oceanic crust in the Urals from Sm-Nd and Rb-Sr systematics. *Earth Planet. Sci. Lett.*, **72**, 389–404.

Fishman, A.M. (2006): Gems in the north Ural and Timan. Geoprint, Syktyvkar, 88 p. (in Russian).

Flores, K.E., Martens, U.C., Harlow, G.E., Bruecker, H.K., Pearson, N.J. (2013): Jadeitite formed during subduction: In situ zircon geochronology constraints from two different tectonic events within the Guatemala Suture Zone. *Earth Planet. Sci. Lett.*, **371–372**, 67–81.

Fu, B., Valley, J.W., Kita, N.T., Spicuzza, M.J., Paton, C., Tsujimori, T., Bröcker, M., Harlow, G.E. (2010): Multiple origins of zircons in jadeitite. *Contrib. Mineral. Petrol.*, **159**, 769–780.

Fu, B., Paul, B., Cliff, J., Bröcker, M., Bulle, F. (2012): O-Hf isotope constraints on the origin of zircon in high-pressure melange blocks and associated matrix rocks from Tinos and Syros, Greece. *Eur. J. Mineral.*, **24**, 277–287.

Gao, J., John, T., Klemd, R., Xiong, X. (2007): Mobilization of Ti–Nb–Ta during subduction: evidence from rutile-bearing dehydration segregations and veins hosted in eclogite, Tianshan, NW China. *Geochim. Cosmochim. Acta*, **71**, 4974–4996.

Garcia-Casco, A., Vega, A.R., Parraga, J.C., Iturralde-Vinent, M.A., Lazaro, C., Quintero, I.B., Agramonte, Y.R., Kröner, A., Cambra, K.N., Millan, G., Torres-Roldan, R.L., Carrasquilla, S. (2009): A new jadeite jade locality (Sierra del Convento, Cuba): first report and some petrological and archeological implications. *Contrib. Mineral. Petrol.*, **158**, 1–16.

Glodny, J., Pease, V. L., Montero, P., Austrheim, H., Rusin, A. I. (2004): Protolith ages of eclogites, Marun-Keu complex, Polar Urals, Russia: implications for the pre- and early Uralian evolution of the northeastern European continental margin., *J. Geol. Soc. Memoir*, **30**, 87–105.

Goldny, J., Austrheim, H., Molina, J.F., Rusin, A., Seward, D. (2003): Rb/Sr record of fluid-rock interaction in eclogites: The Marun-Keu complex, Polar Urals, Russia. *Geochim. Cosmochim. Acta*, **67**, 4353–4371.

Grieco, G., Ferrario, A., Quadt, A.V., Koeppel, V., Mathez, E.A. (2001): The zircon-bearing chromitites of the phlogopite peridotite of Finero (Ivrea zone, Southern Alps): evidence and geochronology of a metasomatized mantle slab. *J. Petrol.*, **42**, 89–101.

Grimes, C.B., John, B.E., Kelemen, P.B., Mazdab, F., Wooden, J. L., Cheadle, M.J., Hanghøj, K., Schwartz, J.J. (2007): The trace element chemistry of zircons from oceanic crust: a method for distinguishing detrital zircon provenance. *Geology*, **35**, 643–646.

Grimes, C. B., John, B. E., Cheadle, M.J., Mazdab, F.K., Wooden, J. L., Swapp, S., Schwartz, J. J. (2009): On the occurrence, trace element geochemistry, and crystallization history of zircon from in situ ocean lithosphere. *Contrib. Mineral. Petrol.*, **158**, 757–783.

Grimes, C.B., Ushikubo, T., John, B.E., Valley, J.W. (2011): Uniformly mantle-like $\delta^{18}O$ in zircons from oceanic plagiogranites and gabbros. *Contrib. Mineral. Petrol.*, **161**, 13–33.

Grimes, C.B., Ushikubo, T., Kozdon, R., Valley, J.W. (2013): Perspectives on the origin of plagiogranite in ophiolites from oxygen isotopes in zircon. *Lithos*, **179**, 48–66.

Gurskaya, L.I. & Smelova, L.V. (2003): PGE mineral formation and the structure of the Syum–Keu Massif (Polar Urals). *Geol. Ore Deposits*, **45**, 309–325. (in Russian).

Harley, S.L., Kelly, N.M., Moller, A. (2007): Zircon behaviour and the thermal histories of mountain chains. *Elements*, **3**, 25–30.

Harlow, G.E. (1994): Jadeitites, albitites and related rocks from the Motagua Fault Zone, Guatemala. *J. Metamorphic Geol.*, **12**, 49–68.

Harlow, G.E. & Sorensen, S.S. (2005): Jade (nephrite and jadeitite) and serpentinite: metasomatic connections. *Int. Geol. Rev.*, **47**, 113–146.

Hoskin, P.W.O. (2005): Trace-element composition of hydrothermal zircon and the alteration of Hadean zircon from the Jack Hills, Australia. *Geochim. Cosmochim. Acta*, **69**, 637–648.

Hou, K.J., Zou, T.R., Qu, X.M., Shi, Y.R., Xie, G.Q. (2007): Laser ablation-MC-ICP-MS technique for Hf isotope microanalysis of zircon and its geological applications. *Acta Petrol. Sin.*, **23**, 2595–2604. (in Chinese with English abstract).

Hu, M.Y., Liao, H.H., Zhan, X.C., Fan, X.T., Wang, G., Jia, Z.R. (2008): Matrix normalization for in-situ multi-element quantitative analysis of zircon in Laser Ablation-Inductively Coupled Plasma Mass Spectrometry. *Chin. J. Anal. Chem.*, **36**, 947–953. (in Chinese with English abstract).

Jiang, Y.H., Liao, S.Y., Yang, W.Z., Shen, W.Z. (2008): An island arc origin of plagiogranites at Oytag, western Kunlun orogen, northwest China: SHRIMP zircon U–Pb chronology, elemental and Sr–Nd–Hf isotopic geochemistry and Paleozoic tectonic implications. *Lithos*, **106**, 323–335.

Kaczmarek, M. A., Muntener, O., Rubatto, D. (2008): Trace element chemistry and U-Pb dating of zircons from oceanic gabbros and their relationship with whole rock composition (Lanzo, Italian Alps). *Contrib. Mineral. Petrol.*, **155**, 295–312.

Kulikova, K.V. (2005): Gabbro complex in the Polar Ural. Autoreferat. Geoprint, Syktyvkar. 19 p. (in Russian).

Li, X.-P., Rahn, M., Bucher, K. (2004): Serpentinites of the Zermatt-Saas ophiolite complex and their texture evolution. *J. Metamorphic Geol.*, **22**, 159–177.

Li, X.H., Li, W.X., Li, Q.L., Wang, X.C., Liu, Y., Yang, Y.H. (2010a): Petrogenesis and tectonic significance of the similar to 850 Ma Gangbian alkaline complex in South China: Evidence from in situ zircon U-Pb dating, Hf-O isotopes and whole-rock geochemistry. *Lithos*, **114**, 1–15.

Li, X-P., Zhang, L-F, Wilde, S.A., Song, B., Liu, X-M. (2010b): Zircons from rodingite in the Western Tianshan serpentinite complex: Mineral chemistry and U–Pb ages define nature and timing of rodingitization. *Lithos*, **118**, 17–34.

Liati, A., Gebauer, D., Fanning, C.M. (2004): The age of ophiolitic rocks of the Hellenides (Vourinos, Pindos, Crete): first U–Pb ion microprobe (SHRIMP) zircon ages. *Chem. Geol.*, **207**, 171–188.

Makeyev, A.B. (1992): Mineralogy of alpine-type ultramafics in the Ural. Nauka, St. Petersburg. 195 p. (in Russian).

Makeyev, A.B., Perevozchikov, B V., Afanacyev, A.K. (1985): Chromite in the Polar Urals. Komi Branch of the Academy of Sciences of USSR, Syktyvkar, Russia, 152 p. (in Russian).

Manning, C.E. (1998): Fluid composition at the blueschist–eclogite transition in the model system Na₂O-MgO-Al₂O₃-SiO₂-H₂O-HCl. *Bull. Suisse Minéral. Pétrogr.*, **78**, 225–242.

— (2004): The chemistry of subduction-zone fluids. *Earth Planet. Sci. Lett.*, **223**, 1–16.

Mattey, D., Lowry, D., Macpherson, C. (1994): Oxygen isotope composition of mantle peridotite. *Earth Planet. Sci. Lett.*, **128**, 231–241.

Meng, F.C., Makeyev, A.B., Yang, J.S., Bai, W.J. (2007): Jadeitite from Syum-Keu ultramafic complex, Polar Urals, Russia. *Acta Petrol. Sin.*, **23**, 2766–2774. (in Chinese with English abstract).

Meng, F.C., Makeyev, A.B., Yang, J.S. (2011): Zircon U–Pb dating of jadeitite from the Syum-Keu ultramafic complex, Polar Urals, Russia: constraints for subduction initiation. *J. Asian Earth Sci.*, **42**, 596–606.

Moldavantsev, Yu.E. & Kazak, A.P. (1977): Khadatinsk ophiolite belt. in "Petrology and metamorphism of ancient ophiolites (Polar Urals and West Sayan as examples)", V.S. Sobolev & N.L. Dobretsov, eds. Nauka, Novosibirsk, 17–37. (in Russian).

Molina, J.F., Austrheim, H., Glodny, J., Rusin, A. (2002): The eclogite of the Marun-Keu complex, Polar Urals (Russia): fluid control on reaction kinetics and metasomatism during high P metamorphism. *Lithos*, **61**, 55–78.

Molina, J.F., Poli, S., Austrheim, H., Glodny, J., Rusin, A. (2004): Eclogite-facies vein systems in the Marun-Keu complex (Polar Urals, Russia): textural, chemical and thermal constraints for patterns of fluid in the lower crust. *Contrib. Mineral. Petrol.*, **147**, 484–504.

Mori, Y., Orihashi, Y., Miyamoto, T., Shimada, K., Shigeno, M., Nishiyama, T. (2011): Origin of zircon in jadeitite from the Nishisonogi metamorphic rocks, Kyushu, Japan. *J. Metamorphic Geol.*, **29**, 673–684.

Morishita, T. (2005): Occurrence and chemical composition of barian feldpars in a jadeitite from the Itoigawa-Ohmi district in the Renge high-P/T-type metamorphic belt, Japan. *Mineral. Mag.*, **69**, 39–52.

Morishita, T., Arai, S., Ishida, Y. (2007): Trace element compositions of jadeite (+omphacite) in jadeitites from the Itoigawa–Ohmi district, Japan: Implications for fluid processes in subduction zones. *Island Arc*, **16**, 40–56.

Peacock, S.M. (1990): Fluid processes in subduction zones. *Science*, **248**, 329–337.

Puchkov, V.N. (2009): The diachronous (step-wise) arc-continent collision in the Urals. *Tectonophysics*, **479**, 175–184.

Qiu, Z.L., Wu, F.Y., Yang, S.F., Zhu, M., Sun, J.F., Yang, P. (2009): Age and genesis of the Myanmar jadeite: constraints from U-Pb ages and Hf isotopes of zircon inclusions. *Chin. Sci. Bull.*, **54**, 658–668.

Robinson, P.T., Trumbull, R.B., Schmitt, A., Yang, J.S., LI, J.W, Zhou, M.F., Erzinger, J, Dare, S., Xiong, F. (2015): The origin and significance of crustal minerals in ophiolitic chromitites and peridotites. *Gondwana Res.*, **27**, 486–506.

Rollinson, H.R. (1993): Using geochemical data: evaluation, presentation, interpretation. London, Longman Group UK, 1–343 p.

Rubatto, D., Gebauer, D., Fanning, M. (1998): Jurassic formation and Eocene subduction of the Zermatt-Saas-Fee ophiolites: implications for the geodynamic evolution of the Central and Western Alps. *Contrib. Mineral. Petrol.*, **132**, 269–287.

Saveliev, A.A., Sharaskin, A.Ja., D'Orazio, M. (1999): Plutonic to volcanic rocks, Voykar ophiolite massif (Polar Urals): structural and geochemical constraints on their origin. *Ofioliti*, **24**, 21–30.

Savelieva, G.N. & Nesbitt, R.W. (1996): A synthesis of the stratigraphic and tectonic setting of the Uralian ophiolites. *J. Geol. Soc.*, **153**, 525–537.

Savelieva, G. N., Suslov, P. V., Larionov, A. N., Berejnaya, N. G. (2006): Age of zircons from chromites in the residual ophiolitic rocks as a reflection of upper mantle magmatic events. *Dokl. Earth Sci.*, **411A**, 1401–1406.

Savelieva, G.N., Batanova, V.G., Berezhnaya, N.A., Presnyakov, S. L., Sobolev, A.V., Skublov, S.G., Belousov, I.A. (2013): Polychronous formation of mantle complexes in ophiolites. *Geotectonics*, **47**, 167–179.

Savelyeva, G.N. & Suslov, P.V. (2014): Structure and composition of mantle peridotites at the boundary with crustal complexes of ophiolites in the Syumkeu massif, Polar Urals. *Geotectonic*, **48**, 347–358.

Scambelluri, M., Fiebig, J., Malaspina, N., Müntener, O., Pettke, T. (2004): Serpentinite subduction: implications for fluid processes and trace-element recycling. *Int. Geol. Rev.*, **46**, 595–613.

Scherer, E., Muenker, C., Klaus, M. (2001): Calibration of the lutetium–hafnium clock. *Science*, **293**, 683–687.

Sharma, M., Wasserburg, G.J., Papanastassiou, D.A., Quick, J.E., Sharkov, E.V., Laz'ko, E.E. (1995): High ¹⁴³Nd/¹⁴⁴Nd in extremely depleted mantle rocks. *Earth Planet. Sci. Lett.*, **135**, 101–114.

Shatsky, V.S., Simonov, V.A., Jagoutz, E., Koz'menko, O.A., Kurenkov, S.A. (2000): New data on the age of eclogites from the Polar Urals. *Dokl. Earth Sci.*, **371A**, 534–538.

Sheng, Y.M., Zheng, Y.F., Chen, R.X., Li, Q.L., Dai, M.N. (2012): Fluid action on zircon growth and recrystallization during quartz veining within UHP eclogite: Insights from U-Pb ages, O-Hf isotopes and trace elements. *Lithos*, **136–139**, 126–144.

Shi, G.H., Cui, W.Y., Tropper, P., Wang, C.Q., Shu, G.M., Yu, H.X. (2003): The petrology of a complex sodic and sodic-calcic amphibole association and its implications for the metasomatic processes in the jadeitite area in northwestern Myanmar, formerly Burma. *Contrib. Mineral. Petrol.*, **145**, 355–376.

Shi, G.H., Stockhert, B., Cui, W.Y. (2005): Kosmochlor and chromian jadeite aggregates from Myanmar area. *Mineral. Mag.*, **69**, 1059–1075.

Shi, G.H., Cui, W.Y., Cao, S.M., Jiang, N., Jian, P., Liu, D.Y., Miao, L. C., Chu, B.B. (2008): Ion microprobe zircon U-Pb age and geochemistry of the Myanmar jadeitite. *J. Geol. Soc.*, **165**, 221–234.

Shi, G.H., Jiang, N., Liu, Y., Wang, X., Zhang, Z.Y., Xu, Y.J. (2009): Zircon Hf isotope signature of the depleted mantle in the Myanmar jadeitite: implications for Mesozoic intra-oceanic subduction between the Eastern Indian Plate and the Burmese Platelet. *Lithos*, **112**, 342–350.

Shi, G.H., Jiang, N., Wang, Y.W., Zhao, X., Wang, X., Li, G.W., Ng, E., Cui, W.Y. (2010): Ba minerals in clinopyroxene rocks from the Myanmar jadeitite area: implications for Ba recycling in subduction zones. *Eur. J. Mineral.*, **22**, 199–214.

Shi, G.H., Zhu, X.K., Deng, J., Mao, Q., Liu, Y.X., Li, G.W. (2011): Spherules with pure iron cores from Myanmar jadeitite: type-I deep-sea spherules? *Geochim. Cosmochim. Acta*, **75**, 1608–1620.

Shi, G.H., Harlow, G.E., Wang, J., Wang, J., Ng, E., Wang, X., Cao, S.M., Cui, W.Y. (2012): Mineralogy of jadeitite and related rocks from Myanmar: a review with new data. *Eur. J. Mineral.*, **24**, 345–370.

Shigeno, M., Mori, Y., Nishiyama, T. (2005): Reaction microtextures in jadeitites from the Nishisonogi metamorphic rocks, Kyushu, Japan. *J. Mineral. Petrol. Sci.*, **100**, 237–246.

Shmelev, V.R. (1991): Ultramafic massif Syum–Keu (Polar Urals). Ekaterinburg, 78 p. (in Russian).

Shmelev, V.R. (2011): Mantle ultrabasites of ophiolite complexes in the Polar Urals: petrogenesis and geodynamic environments. *Petrology*, **19**, 618–640.

Simons, K.K., Harlow, G.E., Sorensen, S.S., Brueckner, H.K., Goldstein, S.L., Hemming, N.G., Langmuir, C.H. (2010): Lithium isotopes in Guatemala and Franciscan HP-LT Rocks: insights into the role of sediment-derived fluids during subduction. *Geochim. Cosmochim. Acta*, **74**, 3621–3641.

Sorensen, S., Harlow, G.E., Rumble, D, III. (2006): The origin of jadeitite-forming subduction-zone fluids: CL-guided SIMS oxygen-isotope and trace-element evidence. *Am. Mineral.*, **91**, 979–996.

Sorensen, S.S., Sisson, V.B., Harlow, G.E., Avé Lallemant, H.G. (2010): Element residence and transport during subduction-zone metasomatism: evidence from a jadeitite-serpentinite contact, Guatemala. *Int. Geol. Rev.*, **52**, 899–940.

Spandler, C., Pettke, T., Hermann, J. (2009): The composition of serpentinite dehydration fluids in subduction zones: an experimental study. *Geochim. Cosmochim. Acta*, **73**(Supplement 1), A1256.

Spandler, C., Pettke, T., Rubatto, D. (2011): Internal and external fluid sources for eclogite-facies veins in the Monviso meta-ophiolite, Western Alps: implications for fluid flow in subduction zones. *J. Petrol.*, **52**, 1207–1236.

Sun, S.S. & McDonough, W.F. (1989): Chemical and isotopic systematics of oceanic basalts: implications for mantle composition and processes. in "Magmatism in the Ocean Basins", A.D. Saunders & M.J. Norry, eds., *Geol. Soc. Spec. Publ.*, **42**, 313–345.

Tenthorey, E. & Hermann, J. (2004): Composition of fluids during serpentinite breakdown in subduction zones: evidence for limited boron mobility. *Geology*, **32**, 865–868.

Tseng, C-Y, Yang, H-J., Yang, H-Y., Liu, D.Y., Wu, C.L., Cheng, C-K., Chen, C-H., Ker, C-M. (2009): Continuity of the North Qilian and North Qinling orogenic belts, central orogenic system of China: Evidence from newly discovered Paleozoic adakitic rocks. *Gondwana Res.*, **16**, 285–293.

Tsujimori, T. & Harlow, G.E. (2012): Petrogenetic relationships between jadeitite and associated high-pressure and low-temperature metamorphic rocks in worldwide jadeitite localities: a review. *Eur. J. Mineral.*, **24**, 371–390.

Tsujimori, T., Liou, J.G., Wooden, J., Miyamoto, T. (2005): U-Pb dating of large zircon in low-temperature jadeitie from the Osayama serpentinite melange, southwest Japan: Insights into the timing of serpentinization. *Int. Geol. Rev.*, **47**, 1048–1057.

Udovkina, N.G. (1985): Eclogites of the SSSR. Nauka Press, Moscow. 285 p. (in Russian).

Ulmer, P. & Trommsdorff, V. (1995): Serpentine stability to mantle depths and subduction-related magmatism. *Science*, **268**, 858–861.

Valley, J.W., Lackey, J.S., Cavosie, A.J., Clechenko, C.C., Spicuzza, M.J., Basei, M.A.S., Bindeman, I.N., Ferreira, V.P., Sial, A.N., King, E.M., Peck, W.H., Sinha, A.K., Wei, C.S. (2005): 4.4 billion years of crustal maturation: oxygen isotopes in magmatic zircon. *Contrib. Mineral. Petrol.*, **150**, 561–580.

Wang, X., Shi, G.H., Qiu, D.F., Wang, J., Cui, W.Y. (2012): Grossular-bearing jadeite omphacite rock in the Myanmar jadeite area: a kind of jadeitized rodingite? *Eur. J. Mineral.*, **24**, 237–246.

Wlison, M. (1989): Igneous petrogenesis. Chapman & Hall, London, 153–190 p.

Yamamoto, S., Komiya, T., Yamamoto, H., Kaneko, Y., Terabayashi, M., Katayama, I., Iizuka, T., Maruyama, S., Yang, J., Hon, Y., Hirata, T. (2013): Recycled crustal zircons from podiform chromitites in the Luobusa ophiolite, southern Tibet. *Island Arc*, **22**, 89–103.

Yui, T-F., Maki, K., Usuki, T., Lan, C-Y., Martens, U., Wu, C-M., Wu, T-W., Liu, J-G. (2010): Genesis of Guatemala jadeitite and related fluid characteristics: insight from zircon. *Chem. Geol.*, **270**, 45–55.

Yui, T. F., Maki, K., Wang, K. L., Lan, C. Y., Usuki, T., Iizuka, Y., Wu, C. M., Wu, T. W., Nishiyama, T., Martens, U., Liou, J. G., Grove, M. (2012): Hf isotope and REE compositions of zircon from jadeitite (Tone, Japan and north of the Motagua fault, Guatemala): implications on jadeitite genesis and possible protoliths. *Eur. J. Mineral.*, **24**, 263–275.

Yui, T. F., Fukuyama, M., Iizuka, Y., Wu, C. M., Wu, T. W., Liou, J. G., Grove, M. (2013): Is Myanmar jadeitite of Jurassic age? A result from incompletely recrystallized inherited zircon. *Lithos*, **160–161**, 268–282.

Zaccarini, F., Stumpfl, E.F., Garuti, G. (2004): Zirconolite and Zr-Th-U minerals in chromitites of the Finero Complex, western Alps, Italy: evidence for carbonatite-type metasomatism in a subcontinental mantle plume. *Can. Mineral.*, **42**, 1825–1845.

Zindler, A. & Hart, S. R. (1986): Chemical geodynamics. *Ann. Rev. Earth. Planet. Sci.*, **14**, 493–571.